Content

I. Characterisation of project and report

Final Technical Report

Reporting institution: Institut für physikalische Chemie,
Universität Graz, A-8010 Graz,
Heinrichstraße 28

Principal investigator and Director of Research Institution

Prof. Dr. Dr. h.c. Otto K r a t k y

Project title:

Small angle X-ray investigation of the structures and interactions of nucleic acids, to acquire basic information on the synthesis of milk proteins.

Grant number: FG-Austria-101

Project number: UR-E3-(60)-7

Dates of research period covered by report:

May 25, 1966 to May 24, 1971

II. Summary

Proteins are those substances which control the living processes by acting as catalysts (accelerators of reactions). No life would be possible without them, and only the intelligent cooperation of thousands of different types of protein-molecules, can guarantee a regular course of life.

It is known that proteins represent folded chainlike molecules in which thousands basic units, the amino acids, are arranged in a beadstringlike fashion. There are 20 types of amino acids, that is 20 "types of beads", and the construction of a protein molecule is characterized, if one knows of how many "beads" it consists, and how the sequence, the "code" of the different types of beads is.

Nature makes also use of such a code. It is represented by the molecules of deoxyribonucleic acid (DNA). These are molecules made up from a chainlike arrangement of 4 different types of basic units, the nucleotides. Now, one has found out, that certain groups of three nucleotides represent the code for one certain amino acid. In the same way in which these triplets of nucleotides in the deoxyribonucleic acid succeed each other, the amino acids corresponding to these triplets will follow each other in the protein molecule to be formed. Therefore a chain of deoxyribonucleic acid is a materialized instruction for the set up of a protein molecule. In the nucleus of the cell, in the "genetic material", the recipes for the construction of all proteins which are being produced in the respective cell are stored.

We get an idea of the tremendous wisdom stored in the genetic material if we hear, that the number of triplets of the human hereditary stock is approximately equal to the number of letters of a library consisting of 1000 volumes with about 500 pages each.

It is clear that changes at the deoxyribonucleic acid molecules, that is changes at the "working instruction" for the production of proteins, can decisevely alter the properties of living beings. Actually we know cases in which a change of one single protein will lead to very serious changes in gross properties. Since during each division of a cell a doubling of the deoxyribonucleic acid molecules representing the code must take place, thereby the total succession of heritage would be changed too. Therefore studies about alterations at the deoxyribonucleic acid are of utmost biological interest. We know actinomycin as well as actinomine to effect deep reaching changes in the control function of DNA, which are recognised biologically in an inhibition of tumor growth too. Even in the animal breeding research one is approaching more and more the possibility to bring about the desired properties not only by selection among the spontaneous mutations, but also by controlled influences upon the hereditary stock.

It is essential for the method of investigation applied, namely the X-ray small angle scattering, that the study is carried out with solutions, in which DNA is allowed to react with the anticancer agent actinomycin or the modell substance of it, namely actinomine.

We shall first outline the results attained with actinomine. The use of DNA degraded by supersonant for this purpose proved successful, because it is only with correspondingly short fragments that an eventual lengthening as a result of the building in of the actinomine molecules can be directly ascertained. We observed a lenghtening of the DNA fragments up to 18 %, whereby on an average one actinomine molecule was bound for every 7.1 pairs. This lengthening came about as a result of winding up of the double helix at the site of binding, simultaneously with an intercalation of the actinomine molecule in the double helix.

In the same way we caused decomposed DNA to react with actinomycin. Furthermore we dealt with the X-ray small angle investigations on t-ribonucleic acid. The function of this kind of nucleid acids could be described by the following indication: certain regions of the genetic information placed within the desoxyribonucleic acid are copied by the messenger-ribonucleic acid. This messenger proceeds into the cystoplasma of a cell and is stored there by substances called Ribosomes. There the protein synthesis takes place. In order to bring the amino acids to their proper places, nature uses a third kind of nucleic acids, the transfer-ribonucleicacids. There is an appertaining t-ribonucleicacid for each kind of aminoacid and called after it. This catches the corresponding aminoacid, activates it and brings it to the proper place of the m-ribonucleicacid. The aminoacids now sitting in the right order side by side, their aggregation to the polypeptid takes place, whereby the protein synthesis is executed principally. To get more detailed informations about the process of activation of amino acids during

protein synthesis, a detailed knowledge of the structure of t-RNA is necessary.

Now we summarize the results of the reported measurements. The scattered intensities from dilute solutions of phenylalanin spezific $t\text{-}RNA_{yeast}$ in 0·05 M Tris-buffer (p_H 7·5) at 17°C have been measured. The radius of gyration R (24·4 Å), the molecular weight M (26 100), the volume V (41 500) and the length L (75 - 76 Å), of the molecule were evaluated. A comparison of the experimental with theoretical scattering curves of different models shows, that the shape of the molecule cannot be interpretated by a simple triaxial body. Scattering curves were calculated for more complicated shapes; an elongated body, which has two different cross sections (diameter 22 Å resp. 36 Å) is equivalent in scattering with the $t\text{-}RNA^{Phe}_{yeast}$ molecule.

The change of conformation of $t\text{-}RNA^{Phe}_{yeast}$ on raising the temperature was studied, too. X-ray-small-angle measurements were done at 40°C, 58°C and 70°C. On increasing the temperature from 17°C to 40°C no significant change in the scattering curve is observed; at higher temperatures the radius of gyration is strongly increased with increasing temperature and at 70°C the molecule has a coil conformation.

Finally we studied various solutions of t-RNA at pH 7.5. Each solution contained only one certain kind of cation. As cations lithium, cesium, barium and spermidin were used. The influence of the ions on the radius of gyration of $tRNA^{Phe}_{yeast}$ was considerable. The value of R was 23·6 Å with Li^+ ions, 26·2 Å with Cs^+ ions and 26·3 Å with Ba^{++} ions.

The transcription of the genetic information of the DNA-base sequences into RNA-structure is performed by the DNA-dependent-RNA-polymerase. Not very much is known about this process of transcription. The investigation of the enzyme and of the enzyme-DNA complex will help to clarify the mechanism of transcription. The enzyme DNA-dependent-RNA-polymerase has been highly purified from E. coli. The encyme exists in a monomer and a dimer form and it is not known, whether both or only one of these forms are enzymatically active. I_n solutions of higher ionic strength the encym exists as monomer, in solutions of lower ionic strength as dimer. Both were investigated by small angle scattering and the size, shape, volume and molecular-weight was determined.

Further the encyme can be split by suitable treatment in different subunits, which are seperated by disc-eletrophoresis. The monomer can be split into a so called core-enzyme and a σ-factor. The core-enzyme was studied, too, and size, shape molecular-weight and volume was determined.

The shape of the dimer is equivalent in scattering to a flat hollow cylinder and therefore a possible model for the process of transcription is the following. The enzyme binds to the DNA in such a way, that it surrounds the DNA strand. Then a local melting process of the DNA-double strand perhaps takes place and RNA is synthetized, while the enzyme runs along the DNA-strand. The investigation of a complex of the enzyme with that short part of DNA strand, which is surrounded by the enzyme, will show whether this model of the transcription process fits well.

III. Detailed Report

A) Introduction

The small-angle X-ray scattering method, which is suitable for determining the size, shape and mass of particles in solution of colloid order of magnitude and the mass per unit of length of elongated particles, should be employed--with regard to the far-reaching problems described in the summary--to establish the following facts.

1) How does actinomycine, the well-known anti-cancer substance with DNA, react? What is the interaction with actinomine, the model substance for actinomycin? In this how do the following factors change

a) the length of the DNA-molecule

b) the mass per unit of length

c) the mean cross-section radius of gyration

d) how are these molecules bound? Are they bound at the surface of the DNA or is there an intercalation?

e) What number of these molecule are bound?

Since high-molecular DNA is too long for length-measurement with the small-angle X-ray method, it finally proved necessary to use a DNA which is degraded by supersonant. Fragments of about 500 Å in length were obtained, which permits the length and its alteration to be measured.

2) What morphology has the t-RNA, which has a so important function as mediator between the code fixed in the DNA and the structure of the corresponding proteins? What is the temperature-

dependence of the t-RNA and its dependence on the counter-ions?

3) DNA-dependent RNA-Polymerase

In which way is the information from the DNA transferred to the RNA, what is the mechanism of the process of transcription? The enzyme which catalyses this process is the DNA-dependent RNA-polymerase and it is not known how this enzyme works. Has this enzyme the shape of a hollow cylinder surrounding the DNA-strand and does the enzyme melt up the base-pairings in the region of DNA, at which the process of transcription takes place? The investigation of the enzyme and its subunits, which have important functions with the transcription, is the first step to clarify these problems.

B) Results, Discussion and Conclusions

1) The Interaction of DNA with Actinomine

The interaction of the actinomycine-antibiotica with the desoxyribonucleid-acid (DNA), found by Kersten, Kersten and Rauen[1] in 1960, works out intra-cellulary in an intense retardation of the transcription step within the protein synthesis[2-5]. The high specifity of this retardation effect for some time led the interest of several teams towards the structure of the actinomycine-DNA-complex resulting during this interaction.

The first to develop a structure model for the complex were Hamilton, Fuller and Reich[6] in 1963. In this model the actinomycine accumulates at the surface of the DNA-helix, thereby forming specific hydrogen-bonds between appropriate groups of the actinomycine-chromophors and appropriate groups of the guanin-bases which are indispensable for the binding of the actinomycine. This model indeed explained the guanin specifity of the actinomycines, but left open the question of the reasons for the unusual hydrodynamic and kinetic behavious of the complex. In 1968 Müller and Crothers[7] published a new proposal of structure basing on thermodynamic, hydrodynamic and kinetic measurements. According to this model the chromophor of the actinomycine intercalates between the base-pairs of the DNA during complexing ("intercalation") and develops its guanin specifity in the first place via electronic interaction with the π -systems of the bases. 1969 Wells[8] showed with the help of sequence isomere synthetic desoxy-polynucleotides of double helical secondary structure that, besides guanin apparently

also the nearest neighbour bases determine the affinity of the DNA for the actinomycines. On the basis of the slide-in model[7] this may easily be understood.

For the investigations leading to the slide-in model some phenoxazon derivates, among others the basic, N-substituted actino-cindiamid actinomin was used as a model compound for the function of the actinomycin chromophor for the compound of the actinomycines to the DNA. This appeared justified sofar as the actinomine showed the same behaviour regarding color effect and selection between desoxy-and ribopolynucleotid at this reciprocal effect as the actinomycines themselves. With the investigations of the interaction of DNA with Actinomycin we for some time could not completely overcome the difficulty, that the scattering curves of the DNA-AM complexes were somewhat falsified by the AM portion dissolved, but not bound to DNA. Dissolved AM yields in the range of DNA scattering a horizontal, though weak, but still measurable contribution to the scattering curve. Its contribution is not determined at first, since we cannot tell immediately by X-ray means, how much of the added AM was bound to DNA. Finally we adopted the method, to substract from the scattering of the solution the solvent which is in dialysis equilibrium with the solution. Measurements of this sort have been carried through mainly in the time since having submitted the IV. annual report. The result are represented in detail in the appendix to this report.

An other way was it to carry out the measurements with a DNA, which had been degraded by means of ultrasound to fractions of 500 Å length and simultanously, to use instead of

actinomycin (AM), the actinomine (A). In this way several disadvantages of the samples measured before could be avoided. First the X-ray small angle method allows only with about 500 Å long particle to determine the length beside the diameter, and secondly the A molecule is considerably smaller than the AM, therefore the contribution to the X-ray scattering of the total system of the A molecules dissolved but not bound to DNA is considerably less. Besides the A has, unlike the AM, in solution no more tendency to form aggregates which can lead to a precipitation of the AM-DNS complex. In order to avoid the uncertainty in the evaluation of the measurements due to the not bound A fraction in solution, we work on principle only with solutions saturated with A. That is to every DNA solution an amount of dry A was added, until a deposit formed at the bottom. In this way we made sure, that all DNA molecules of the solution are loaded fully with A. Furthermore, by measuring the scattering of a saturated A solution, the correct solvent scattering could be determined and subtracted from the scattering of the total system.

For the X-ray small angle measurements, concentration series of the sodium DNA solution, and the DNA-A solution of the same DNA concent were prepared, starting out from the master solution with 1,44 % DNA (phosphate buffer pH7, 0,01 m NaCl). Dilution steps 1:1 were used down to 1/32 of the starting concentration.

Already the first orienting measurements have shown, that the scattering curves of higher concentrations show significant interference maxima in about the middle range of the curve (Fig. 1). Only after an enhancement of the NaCl concentration to 0,30 m we obviously obtain the scattering curves without

interference peaks (Fig. 2). In order to obtain the total radius of gyration R of the particle, the scattering curve inflicted with the collimation error was extrapolated towards zero concentration. For each abszissa value, all ordinates of the scattering curve normalized to concentration c = 1 were plotted in dependence of c. Thereby a quadratic dependence of the intensities on c was obtained. These extrapolated scattering curves (one for Na-DNA and one for DNA-A) were corrected for the collimation error (Fig. 3) and evaluated. The molecule of the degraded Na-DNA has a total radius of gyration R = 148 Å, that of DNA loaded maximally with A a radius of gyration R = 166,4 Å (Fig. 4). From the cross section scattering curve we obtain a R_q of 8,4 Å for the not loaded DNA, a R_q of 8,00 Å for the DNA molecule loaded with A (Fig. 5). This means for the loaded DNA an elongation from about 510 Å to 575 Å, with a simultanous decrease of the radius of the circular cross section of the molecule from r = 11,8 Å to 10,3 Å.

Very important is the observation that much too high a molecular weight is found from the absolute scattering intensity at zero angle. As a result of this all statements previously made appear uncertain, and it was necessary to get to the bottom of this peculiar effect. An explanation finally resulted from the study of the so-called cross-section factor extended to extremely small angles (Fig. 6). A quantitative interpretation finally led by compulsion to the idea that the rod-shaped DNA particles are surrounded by an ion shell, which has the form of a hollow cylinder and seems to be responsible for the scattering effect (Fig. 7). It is only the inclusion of

this ion shell in all further calculations which renders possible a clarification of the situation in the binding of actinomin. It was now also possible to calculate that with full saturation with actinomin there was a lengthening of the DNA by 18 %, and the mass of the bound actinomin could be calculated: on an average there is accordingly one bound actinomin molecule for every 7.1 base pairs.

2) On the Conformation of Phenylalanine Specific Transfer RNA

Results

To get mor detailed information about the process of activation of amino acids during protein synthesis by the tRNA-aminoacyl synthetase system a detailed knowledge of the structure of tRNA is necessary. Although several sequences (= primary structures) of tRNAs are known, one cannot derive secondary and tertiary structures from these sequences. In this respect the situation is similar to that in the protein field.

Previously a mixture of tRNAs [9] as well as purified $tRNA^{Ala}$ (yeast) [10] and $tRNA^{Val\ I}$ (E.coli) [11] were investigated by the X-ray small angle method. In these investigations the temperature dependence of the scattering was not studied. We carried out our measurements with a pure species of $tRNA^{Phe}$ (yeast) over a wide temperature range.

Size and Shape of $tRNA^{Phe}$ (yeast) at 17°

In Fig. 8 the inner portion of the experimental scattering curve is shown at different concentrations. The scattering curves have a Gaussian shape at small angles as shown in Fig. 9. At higher concentrations the scattered intensity in the inner portion is significantly lowered by interference effects. It can be eliminated in the manner indicated in Fig. 9. Practically the same values for $\bar{R}$ are found by the plot of Fig. 10.

After elimination of the collimation effect the correct radius of gyration R was determined to be 24.4 ($\pm$ 0.3) Å. Additional 10 mM Mg^{++} in the solution did not cause a significant change in the scattering curves.

From I_o/P_o and $\bar{v}_1$ (0·54) we could calculate a molecular weight of 26 100. The volume V of the particles in solution can be calculated from the invariant Q of the scattering curve and I_o. We find V = 41 500 ($\pm$ 1200) $Å^3$.

From the molecular weight M and the partial specific volume $\bar{v}$ the volume of the unswollen particle results directly. The comparison with the value obtained from the invariant gives the degree of swelling q = 1.77. This value corresponds to 0.42 g H_2O per 1 g $tRNA^{Phe}$ (yeast).

From the Guinier plot of the cross-sectional factor the radius of gyration of the cross-section R_q was found to be 11.0 Å.

If R and R_q are known for the length of the particle we obtain the value of 75 Å. There is another way to calculate the length of a particle that is from the molecular weight M and the mass per 1 Å length (M/1 Å) of the particle. M/1 Å was found to be 344.

By dividing M (26 100) by M/1 Å (344) a value of 76 Å is obtained for the length. Since this value is in good agreement with the value calculated from the radii of gyration, the shape of the $tRNA^{Phe}$ (yeast) molecule is approximated well by a cylindrical body which has a length of 75 - 76 Å.

The comparison of the experimental scattering curve with the calculated curves of triaxial bodies, led to a ratio of diameter to length of about 1:2.5 (Fig. 11), assuming rotational cylinders.

A more detailed determination of the shape shows that the $tRNA^{Phe}$ (yeast) molecule cannot be interpreted by a cylinder of an uniform cross-section. The experimental scattering curves differ clearly from the theoretical curves of simple cylinders; in particular the curves of the cross-section show in the Guinier plot two different regions. The inner, steeper portion yields a R_{q1}-value of 11.0 Å, while the outer, flatter portion yields R_{q2}-values in the range of 9.5 Å to 9.1 Å as shown in Fig. 12.

This indicates that there are two portions of the molecule with different cross-sections; therefore we calculated the scattering curves for a number of different models. Due to the limitations of computer programs available, only ellipsoids instead of cylinders could be used. This substitution however should not substantially affect results.

The best agreement with the experimental curve is given by the models shown in Fig. 11. It consists of 3 ellipsoids with their main axes arranged parallel. The axes of the large ellipsoid have the following dimensions (in Å): a = 11,

b = 11, c = 46, and the two small ellipsoids have dimensions of a = 9, b = 9, c = 24. The radius of gyration and the volume of this model is in good agreement with the experimental values. Assuming the same radius of gyration the long axes ellipsoids are longer than the corresponding lengths of cylinders. The scattering curve of the model is in agreement with the experimental curve (Fig. 11).

Change of conformation of $tRNA^{Phe}$ (yeast) on increasing temperature

It is not possible to obtain exact information on the actual shape of the molecule by the method of X-ray small angle scattering, but the method is highly sensitive with respect to changes of conformation of a molecule. We therefore studied the conformational change of tRNA, which accompanies the melting of base pairs. In Fig. 13 the optical-melting curve of the $tRNA^{Phe}$ (yeast) in 0.4 M phosphate buffer at pH 7.0 is given. The T_m-value lies at 57°.

The small angle scattering measurements were done at 17°, 40°, 58° and 70° in 0.05 M Tris buffer at pH 7.5.

In Fig. 13 the radii of gyration (after elimination of the collimation effect) too are plotted versus the temperature, and the melting curve of $tRNA^{Phe}$ (yeast) is shown. Both curves exhibit similar shapes. The change in conformation at the melting temperature goes parallel with an expansion of the molecule.

The scattering curve of the $tRNA^{Phe}$ (yeast) at 70° has a course typical for relatively short chains. The scattering

curve of a coiled molecule in solution is known to be composed of three portions [12 bis 14]: the inner portion according to a Gaussian curve is due to the coil as a whole. The middle portion obeys a $1/(2\theta)^2$ law and the exterior a $1/2\theta$ law. The transition point between these two outer portions is most distinct if $I \times (2\theta)^2$ is plotted versus 2θ, as seen in Fig. 14. From the position of this transition point, one can draw conclusions on the average curvature of the chain, which is defined by the "persistence length". According to the equation

$$\bar{a} = 2 \times 2.3 \times \frac{\lambda}{4\pi} \times \frac{1}{(2\theta)^*}$$

a persistence-length $\bar{a}$ of 30 Å can be calculated from the $(2\theta)^*$ abscissa-value of the transition point.

Discussion and Conclusions

The observed radius of gyration R = 24.4 Å for $tRNA^{Phe}$ (yeast) at room temperature is close to the values obtained by Lake and Beeman [9] (R = 23.5 Å for bulk tRNA from yeast at 22.5°) and Krigbaum and Godwin[10] R = 23.9 Å for bulk tRNA from yeast and R = 23.2 Å for $tRNA^{Ala}$ (yeast) . We have compared our scattering curves with those of Connors et al.[15] and Ninio et al.[16]. Our scattering curve agrees well with the curves of Connors et al., only the low peak at a Bragg spacing of 29 Å is not present in the scattering curves of Connors et al. Also the radii of gyration (R = 23.5 - 25 Å) and the dimensions 25 by 35 by 85 Å named by the authors agree with our value (R = 24.4 and 25.1 Å) and the dimensions of our model composed of

ellipsoids (diameters 22 and 36 Å, length 92 Å).

The scattering curve of Ninio et al., however, deviates especially in the tail end from the scattering curves of Connors et al. and of ours; the radius of gyration of 25 Å corresponds to our value.

The fact that two different cross sections are observed, rules out a simple triaxial body for the molecule. Models like a symmetrical H-model[9] or almost symmetrical arrangements by folding all arms together[17] can be excluded, whereas others are compatible with the results[16,18,19].

The two different cross sections might be interpreted in the following way: the diameter of 22 Å corresponds to the diameter of a single Watson and Crick helix and can be attributed to the anticodon arm. The cross section of 36 Å diameter is in agreement with a compact part of the molecule where parts of the cloverleaf are folded together.

The cross sections of the model formed by folding together dihydrouridine loop, T-Ψ-C-G loop and C-C-A end[18] fit with the above data. Also the length/overall width ratio (2.5) is in agreement with that model. The overall radius of gyration (24.4 Å) is, however, larger than expected for the model. One should however take into consideration that a highly solvated poly-anion with an ionic layer around itself might show anomalies[20-22] which do not allow a direct correlation between measured and calculated R-values. A correction for the kind of ions and the sphere of hydration might be necessary[23].

The molecular weight as determined from the X-ray scattering is 26 100, as compared to the value from the known sequence of 24 890 (without counter ions). The volume (4.1×10^4 Å^3) of the

particle in solution is in good agreement with the data obtained from X-ray diffraction work on single crystals[24]. From the size of the unit cell and the number of molecules in it, a volume per molecule of 3.84×10^4 Å^3 is calculated[24].

The temperature dependency of the scattering data can easily be explained by a transformation of the highly structured conformation of $tRNA^{Phe}$ (yeast) into a random coil. This unfolding is also reflected in a strong increase in viscosity as determined by Henley et al.[25].

3) Influence of counterions on the radius of gyration of Phenylalanine Specific Transfer RNA

Results

The comparison of the experimental small angle X-ray data with those calculated for a particular model involves a difficult problem. The experimental studies are carried out in solution and the influence of the solvent, the counterions and additional electrolytes on the radius of gyration is not well known.

Since the problem of the structure of the water shell could not be completely clarified even with simple ions[26], the theoretical treatment of the water shell and hydration presents very great difficulties with a polyelectrolyte such as tRNA.

Therefore the influence of the water and ion cloud shell is frequently ignored; some authors[15,16] assign one univalent ion to each phosphate group of the tRNA molecule for the calculation.

Theoretically, polyions have discrete charged groups, and for many calculations it is assumed that counterions are bound only to these discrete groups. In real polyions, however, a diffuse atmosphere of counterions in which the distribution of the counterions fluctuates must be assumed[26]. A theoretical treatment of this problem, based upon a geometric concept, was given by Luzzati et al.[27].

In order to compare the experimental data with the data calculated for the various suggested models it seemed important to discover more about the influence of both hydration and the binding of counterions. Consequently we investigated $tRNA^{Phe}$ in solution in several cationic forms.

Similar studies were effected by Luzzati et al.[27] and Bram[28] on DNA molecules; the authors determined the mass per unit length and the radius of gyration of the cross-section of DNA by using various counterions. The results obtained by the two groups are not in mutual agreement, as is discussed in detail by Eisenberg and Cohen[29].

Preparation of $tRNA^{Phe}$ (yeast) with a certain cation

77 mg of $tRNA^{Phe}$ from yeast prepared as described by Holley et al.[30] was dissolved in 20 ml of double-distilled water. 5 ml aliquots were dialyzed once against 0.4 M sodium phosphate pH 7.0, twice against bidistilled water, once against 0.4 M sodium phosphate pH 7.0, twice against bidstilled water, three times against 0.1 N of univalent cation (0.1 N LiCl or 0.1 N CsCl), or three times against 0.01 N divalent cation (0.01 N $BaCl_2$ or 0.01 N spermidine chloride) solution and three

times against double-distilled water to remove excess ions.

The dialyzed solution was freed of dust by passage along sintered glass and finally lyophilised.

Solutions Used for the Small Angle Measurements

The freeze-dried samples of $tRNA^{Phe}$, each containing only one certain kind of cation, were dissolved in the following buffers: Li-tRNA in 0.05 M citric acid/LiOH pH 7.5, additional 0.1 M LiCl; Cs-tRNA in 0.05 M citric acid/CsOH pH 7.5, additional 0.1 M CsCl; Ba-tRNA in 0.05 M Tris, pH 7.5, in a second series 0.05 M $BaCl_2$ was added; spermidine-tRNA in 0.05 M Tris, pH 7.5, in a second series 0.05 M spermidine chloride was added.

With each type of $tRNA^{Phe}$ (Li-tRNA, Cs-tRNA, Ba-tRNA, spermidine-tRNA) several series were investigated, whereby the concentration of tRNA was varied from 2 mg/ml up to 20 mg/ml.

The apparent radii of gyration obtained from the slope of the slit-smeared curves are summarized in Table 1. (The scattering curves of spermidine tRNA showed a divergent behaviour. During X-ray irradiation, evolution of gas was observed and apparently some decomposition had occurred. Therefore a more detailed evaluation had to be abandoned.)

In Fig. 15 the apparent radii of gyration ($\bar{R}$), summarized in Table 1, are plotted against the concentration of the corresponding $tRNA^{Phe}$ in solution. It can be clearly seen that the radius of gyration with Li^+ as cation is markedly smaller than with the heavy cations Cs^+ and Ba^{++}. Comparison of the scattering curves of Ba-tRNA with and without the addition of

$BaCl_2$ shows that, while the dependence of the $\bar{R}$-values on the concentration is lessened by the addition of 0.05 $BaCl_2$, the values obtained by extrapolation to zero concentration are almost identical.

In Table 2 the ions used and their atomic weights are given, as well as the radii of gyration obtained after slit-correction and extrapolation to zero concentration (see Fig.5). For comparison the R-value which we found in our first investigations[18,19] of $tRNA^{Phe}$ using a mixture of K^+ and Mg^{++} ions is also given.

The $tRNA^{Phe}$ consists of 76 nucleotides. If one assumes that one univalent cation belongs to the phosphate group of each nucleotide and one more ion to the phosphate group localized at the 5' end of the tRNA chain, 77 univalent ions would belong to each tRNA molecule. Assuming further that these ions belong to the molecule, the amounts of weight given in Table 2 are to be added to the molecular weight of the $tRNA^{Phe}$ of 24 890 calculated from the sequence. It seems that the radius of gyration increases not with the equivalent weights of the cations, but with their atomic weights since the R-values obtained with Cs^+ and Ba^{++} ions are nearly identical, as are also the atomic weights of the two ions.

In Fig. 16 the slit-corrected values of the radii of gyration which we obtained are plotted against the atomic weight of the cations used. The R-value obtained with Cs^+ or Ba^{++} as counterion is about 10 % higher than that obtained with Li^+.

In order to estimate whether this increase in the R-value is plausible, we carried out the following rough calculation. The $tRNA^{Phe}$ molecule was approximated by a cylinder of axial

ratio 1:2.5, and it was assumed that, for example, 77 cesium ions per $tRNA^{Phe}$ molecule were uniformly distributed in a shell of 2 Å thickness (the round value of the ionic radius) around this cylinder. From this rough calculation an increase in the R-value of 7 % results from the transition from Li-tRNA to Cs-tRNA.

Discussion and Conclusions

The present work shows clearly that the influence of the solvent, and especially that of the ions, must in no case be disregarded when polyelectrolytes (in the present instance tRNA) are investigated in solution. The work of Luzzati[27] and Bram[28] also clearly shows the great influence of the ions on the cross-section of DNA molecules. Eisenberg and Cohen[29] likewise indicate that very exact measurements are necessary in order to get a better influence of the ions was considerable; the value of R was, for instance, 23.6 Å with Li^+ ions and 26.2 Å with Cs^+ ions. This increase in the R-value lies roughly in the magnitude to be expected if one assumes that one univalent ion belongs to each phosphate group. This assumption is also usually made when experimental data are compared with the data calculated from the atomic coordinates of a proposed model. That this can be regarded only as a rough approximation is shown by the fact that the value of the radius of gyration is not dependent on the equivalent weight but on the atomic weight of the cation (see Table 2). If it were dependent on the equivalent weight a smaller R-value would be expected for Ba^{++}-tRNA than for Cs^+-tRNA. In point of fact, however, we find almost the

same R-value for Cs^{+}- and Ba^{++}-tRNA.

This result clearly shows that hydration must also be an essential factor. Satisfactory theoretical treatment of the structure of the water shell has not yet been successful even with simple ions[26], and, obviously, more complex polyelectrolytes will present even greater problems.

Finally it should be noted that the type of solvent used naturally influences not only the radius of gyration and molecular weight but also the entire scattering curve, especially the tail-end. It is thus also difficult to carry out detailed determinations of the conformation of the tRNA molecule by means of comparison of the experimental curves with scattering curves calculated from the atomic coordinates. We shall at present have to content ourselves with obtaining an overall shape as long as the influence of the counterions and hydration cannot be presicely accounted for.

Appendix

I. The Interaction of degraded DNA with Actinomycin (AM)

A) Introduction

From the beginning of our project we have studied the interaction of deoxyribonucleic acid (DNA) with the antibiotic actinomycin. Actinomycin binds to DNA and blocks the synthesis of messenger ribonucleic acid[1-5]. Models for the structure of the DNA-actinomycin complex were developed first by Hamilton, Fuller and Reich[6], which proposed hydrogen-binding of the actinomycin chromophor to the outside of the DNA helix, and more recently by Müller and Crothers[7] which assumed intercalation of the chromophor between the bases of the helix, similar to the model for the DNA-proflavine interaction as proposed by Lerman[31].

We had begun our investigations with a study of the interaction of native NaDNA with actinomycin C_3. The results of that investigation have been reported mainly in the 1st Annual Report. However, those measurements did not satisfy completely as the use of native DNA brought about some serious problems. Moreover we did not have the solutions in dialysis equilibrium with the solvent so all measurements were afflicted with indefinite uncertainties.

However, we have learnt from that and the study of the interaction of DNA with actinomine was already performed with DNA that had been degraded by ultrasonic treatment to a molecular weight of about 10^5. The final results of that study have been

reported in the 4th Annual Report[32].

In the following we shall present the results of an investigation of the interaction of sonicated NaDNA with actinomycin C_3 again. Apart from the use of sonicated instead of native DNA we had now all solutions in dialysis equilibrium with the solvent, so the results should be much more reliable than those obtained from the first measurements.

B) Materials and Methods

Small angle X-ray measurements were carried out with samples of sonicated calf thymus DNA in BPES buffer. The mean molecular weight of the NaDNA was about $1{,}2 \times 10^5$. Some samples were charged with definite amounts of actinomycin C_3 and dialyzed extensively against BPES buffer containing the equilibrium concentration of free actinomycin[7]. The NaDNA samples not charged with actinomycin were brought into dialysis equilibrium with pure BPES buffer. Final concentration of NaDNA was 8.7 mg/ml and 4.35 mg/ml, respectively.

Scattering experiments were carried out very carefully. All curves were measured repeatedly. The total number of pulses registered for each point of the scattering curve varied from 3 x 40000 to 8 x 40000. The experimental data were punched on a paper tape and evaluated by means of the computer program described in the 4th Annual Report.

Smoothing of the experimental curves was achieved by approximating them by polynomials of the kind

$$f(x) = \sum_{i=1}^{10} a_i \, x^{i-5}$$

which turned out to be very useful for this scattering problem. The coefficients of the polynomials were calculated from the experimental data by the weighted least square method. This was performed by a computer program that has been developed especially for this problem. As this program takes over the data directly from the evaluation program already described and is coupled to the comined desmearing and monochromatization program[33,34] it was possible to perform the complete evaluation of the experimental data in a single run. Computer time for the evaluation of one scattering curve was about half a minute for the UNIVAC 494.

C) Results

The final scattering curves for the different samples are shown in fig. 17. The curves are presented in a plot log $Ix2\theta$ versus $(2\theta)^2$ as it is usual for rod-like particles. The amount of bound actinomycin which is expressed by r, the number of actinomycin molecules bound per base pair, varies from 0 (bottom) to 0.16 (top). Within this range all curves appear to be very similar to each other.

From the slope of the curves at small angles as indicated by the straight lines in fig.17 the radius of gyration of the cross section R_c was determined for the different samples in the usual way. The obtained values are summarized in Table 3. Where control measurements had been performed the average was taken finally over all results. The averaged values are also reported in Table 3.

As recently stated by Eisenberg and Cohen[29] the equations

$$M/\mathring{A} = \frac{27.3\ (Ix2\theta)_o\ a^2}{P_o c_1\ D(z_1-\bar{v}_1\rho_2)^2} \qquad (1)$$

is only applicable to two-component systems. In the case of a multi-componentsystem consisting of an undiffusable polyelectrolyte (subscript 1), of the principal solvent water (subscript 2) and of n-2 diffusable low molecular weight components (subscript i) one has to replace the expression $(z_1 - \bar{v}_1\rho_2)$ by the more general expression $(\delta\rho/\delta c_1)_\mu$, the electron density increment at constant chemical potentials of all components excepted component 1.

However, we shall demonstrate in the following that by only replacing the partial specific volume $\bar{v}_1$ by the apparent partial specific volume $\bar{v}_1$ which will be defined below equation (1) becomes applicable to multi-component systems too in good approximation.

The electron density increment is defined by

$$(\delta\rho/\delta c_1)_\mu = z_1 - \bar{v}_1 - \sum_3^n \xi_i(z_i - \bar{v}_i\rho) \qquad (2)$$

Here z_i = moles of electrons per gram of diffusable component i, $\bar{v}_i$ = partial specific volume of component i; ξ_i is the socalled interaction parameter of component i, defined by $\xi_i = -(\delta w_i/\delta w_1)_\mu$, the weight of component i (in grams) to be removed from the solution per gram of component 1 added, in order to maintain constancy of all components excepting component 1.

As the partial specific volume of component 1 is defined by

$$\bar{v}_1 = 1 - (\delta d/\delta c_1)_\mu - \sum_3^n \xi_i(1 - \bar{v}_i d) \quad /d \qquad (3)$$

equation (2) can be rewritten as

$$(\delta\rho/\delta c_1)_\mu = z_1 - z\left[1 - (\delta d/\delta c_1)_\mu\right] - \sum_3^n \xi_i(z_i - z) \qquad (4)$$

By inserting the apparent partial specific volume $\bar{v}_1'$ of component 1 which is defined by

$$\bar{v}_1' = \left[1 - (\delta d/\delta c_1)_\mu\right]/d \qquad (5)$$

we obtain

$$(\delta\rho/\delta c_1)_\mu = z_1 - \bar{v}_1'\rho - \sum_3^n \xi_i(z_i - z) \qquad (6)$$

Here d = density of the solvent containing all components excepted component 1, z = moles of electrons per gram of this solvent. The quantity $(\delta d/\delta c_1)_\mu$ is the density increment at constant chemical potentials of all components excepted component 1. It can be determined by a precise measurement of the densities of the solvent and of the solution containing component 1 in well-known concentration and being in dialysis equilibrium with the solvent.

The interaction parameters ξ_i must be determined by separate experiments such as the analytical determination of the differences of salt concentration between the solution and the solvent. As this would have been very difficult in the case of BPES buffer we tried to estimate the error involved by omitting the term $\Sigma\xi_i(z_i - z)$ from equation (6).

With $z_1 = 0.514$, $\rho = 0.557$ and $\bar{v}_1' = 0.557$ cm^3/g as determined by the method described in the 2nd Annual Report we obtair from the first two terms on the right-hand side of equation (6) a value of $(\delta\rho/\delta c_1)_\mu = 0.204$. From the data for the system NaDNA-NaCl as given by Cohen and Eisenberg[37] we calculate $\xi_{NaCl} = 0.043$.

From this and $z_{NaCl} = 0.479$ and $z_{BPES} = 0.554$ it follows $\xi_i(z_i - z) = 0.003$ which is only about 1.5 % of $(\delta\rho/\delta c_1)_\mu$. The value of 0.003 refers to about 0.2 M NaCl. We may now assume that the corresponding values for the other diffusable components of BPES buffer if considered isolated are of similar magnitude. Thus for the system NaDNA - BPES buffer if considered as a whole the term $\Sigma\xi_i(z_i - z)$ will probably be of the same magnitude and its contribution to $(\delta\rho/\delta c_1)_\mu$ will not exceed 1.5%. This seems to be small enough to justify neglecting the term in first approximation.

So far we were concerned only with NaDNA not charged with actinomycin. For the determination of the mass per unit length of the NaDNA charged with actinomycin we may assume additivity of the apparent partial specific volume of NaDNA and that of actinomycin, which is 0.786 cm^3/g [38]. The apparent partial specific volume of the complex can be calculated as

$$\bar{v}'_{D+A} = \frac{\bar{v}'_D M_D + r \bar{v}'_A M_A}{M_D + r M_A} \qquad (7)$$

The subscripts D and A refer to NaDNA and actinomycin, respectively. Inserting $r = 0.16$, $M_D = 661.9$, the mean molecular weight of a nucleotide pair and $M_A = 1280$ we calculate $\bar{v}'_{D+A} = 0.611$ cm^3/g. An identical value was obtained from an experimental determination.

In the same way z_{D+A} can be calculated from $z_D = 0.514$ and $z_A = 0.534$. For $r = 0.16$ we obtain $z_{D+A} = 0.519$. As the amount of free actinomycin in the solvent is very low it does not influence the electrondensity of the solvent to an appreciable extent. Thus the electrondensity increment of the complex can be calculated as 0.178.

The concentration of the complex is by a factor of $(M_D+rM_A)/M_D$ higher than the concentration c_D of NaDNA. For r = 0.16 the factor is 1.309. Now it turned out that 1.309 x $(0.178)^2$ is equal to 0.0415, the value of $(\delta\rho/\delta c_D)^2$ as derived above for NaDNA not charged with actinomycin. In the same way almost identical values for the expression $(M_D + r\,M_A)\,(\delta\rho/\rho c_{D-A})^2/M_D$ were calculated for values of r other than 0.16.

Therefore independently of the amount of actinomycin bound to NaDNA the determination of the mass per unit length of the different samples could be based on the general formula

$$M/\mathring{A} = \frac{27.3\ (Ix2\theta)_o\ a^2}{P_o c_D D\ (z_D - \bar{v}'_D\rho)^2} \qquad (8)$$

where all quantities marked with the subscript D refer to pure NaDNA.

A summary of the obtained values for $M/\mathring{A}$ is given in Table 4.

D) Discussion

Before we discuss our results in detail some general remarks might be useful. Our measurements presented in this report are restricted to the mere cross section region of the scattering curves of DNA. By our previous measurements [32] it had turned out that this region which begins at Bragg spacings of about 100 $\mathring{A}$ is practically not sensitive to the concentration of dissolved DNA, so we could perform all present measurements with solutions of relatively high concentrations of 8.7 mg/ml and 4.35 mg/ml.

On the other hand, as reported earlier[32] the scattering

curves of sonicated NaDNA show a strong dependence upon polymer concentration at Bragg spacings larger than 100 Å, thus one is forced to measure an extended concentration series when studying that region of the curves. In the 4th Annual Report we had interpreted the results obtained from an investigation of that region at very small angles by the assumption of an ion shell surrounding the DNA. The influence of this ion shell on the scattering curve could be detected only with solutions of concentrations much below those used by us now. This implies that we cannot present new data referring to this ion shell now and that we shall interpret all our new results as if there were not such an ion shell at all.

The radius of gyration of the cross section of pure NaDNA of 8.7 Å as given in Table 3 is larger than the corresponding value of 8.4 Å obtained by our previous measurements[32]. A value of 8.4 Å was also found by Luzzati et al.[20,27,35]. On the other hand, Bram and Beeman[36] very recently reported a value of about 9 Å as radius of gyration of the cross section of pure NaDNA. These results are rather contrary to each other.

But there is a second discrepancy. Bram and Beeman found two cross section regions in their scattering curves, one at smaller angles yielding the value of 9 Å mentioned above and a second region at larger angles from which they derived a radius of gyration of 7.8 Å. On the contrary all measurements before Bram and Beeman had led to a single cross section region corresponding to the radius of gyration of 8.4 Å.

However, we believe that our experiences won from the investigations presented in this paper will clear up these discrep-

ancies. The cross section region of the scattering curves of DNA seems to be rather sensitive to the degree of smoothing the experimental curves. When we smooth the experimental curves more rigorously we obtain values smaller than 8.7 Å, when we smooth them less then we find larger values. As can be seen from fig. 17 all scattering curves deviate at larger angles from the straight lines. Obviously the contiguous region corresponds to the second cross section region found by Bram and Beeman. In our curves this region is somewhat bent and approcimation by a straight line is not possible over a longer range. However, when we draw straight lines through the points which are plotted in fig. 17 we obtain a value of 8.2 Å as second radius of gyration of pure NaDNA. This value is now slightly larger than the corresponding radius found by Bram and Beeman, but this seems reasonable with respect to the fact that the slope of this region of the scattering curve becomes steeper when the experimental data are smoothed more rigorously. If we take the average over the two radii found by us a mean value of 8.45 Å is obtained and from the data given by Bram and Beeman a mean radius of gyration of 8.4 Å can be calculated. These are practically the same values as found by Luzzati and by the previous measurements in our group.

From these results we conclude that a rigorous smoothing of the experimental curves is able to obscure the existence of two cross section regions in the final curves and leads to a single cross section region, whose slope is approximately the average of the slopes of the inner and outer cross section region of a less smoothed curve. As compared with the curves obtained by Bram and Beeman the curves shown in fig. 17 seem to be smoothed

somewhat more rigorously, whereas the curves reported earlier by us and by Luzzati are obviously very rigorously smoothed.

As our present study is concerned especially with finding up the differences between very similar curves it was necessary to smooth all experimental curves in the same way. This was achieved by the procedure described in a previous section. Only by this procedure it was guaranteed that the results obtained for different samples are comparable with each other and that differences between the curves for several degrees of charging with actinomycin are really due to the bound actinomycin and not due to smoothing effects. So the radii of gyration as given in Table 3 are accurate to ± 0.1 Å as compared with each other, the absolute error, however, might be much larger.

The dependence of the radius of gyration of the cross section upon the amount of bound actinomycin is shown in fig.18. This figure implies an approximately linear decrease of R_c with increasing degree of charging. The difference between the radius of gyration of the uncharged sample and that of r = 0.16 is 0.6 Å. A similar decrease, namely 0.4 Å for r = 0.14 was found for the system NaDNA-actinomine by our previous measurements[32]. Our result is also in qualitative agreement with that obtained by Luzzati and coworkers[20,27,35] for the DNA-proflavine interaction.

A decrease of R_c with increasing r is incompatible with any model proposing mere binding of the actinomycin to the outside of the DNA helix[6], but it is in very good agreement with the intercalation model[7]. This model implies an intercalation of the actinomycin chromophor between the bases adjacent to a GC -

pair and a specifical interaction of the peptide rings with the DNA backbone, one ring interacting with each strand of the double helix. In the first case, binding of the actinomycin to the outside of the helix, the radius of gyration of the cross section must increase with the amount of bound actinomycin. For the intercalation model a decrease of R_c is expected for two reasons : the radius of gyration can be reduced by an additional mass brought nearer to the center of gravity and binding of the chromophor may produce a distortion of the helix.

If the decrease of R_c is mainly due to the additional mass brought nearer to the center of gravity the effect should be larger with the actinomine which lacks the peptide rings that by interaction with the DNA backbone would extend to the surface of the helix. Indeed the effect is even somewhat larger with the actinomycin. Thus we may conclude that the decrease of the radius of gyration is mainly due to the helix distortion. The extent of the distortion can be roughly estimated by the following considerations. Neglecting the additional volume introduced by the bound actinomycin we assume that the volume of the DNA helix itself does not alter with charging. Then a contraction of the cross section of the helix, as indicated by the decrease of R_c, must be compensated by a stretching of the helix. The elongation l_A of the helix per actinomycin bound can be easily calculated from

$$l_A = \frac{3.36}{r} \left(\frac{R_{c,o}^2}{R_{c,r}^2} - 1 \right) \qquad (9)$$

In this formula the subscripts o and r refer to the uncharged and

charged NaDNA, respectively. 3.36 Å is the base-pair spacing for the B structure[39]. From the radii of gyration obtained for r = 0, 0.05, 0.1 and 0.16 an elongation per bound actinomycin of about 3.2 Å is calculated. Considering the too idealized assumptions on which the calculation is based the obtained value is in good agreement with the elongation of 4.5 Å as derived from hydrodynamic measurements[7].

In Table 4 we have reported a value of 207 as mass per unit length of pure NaDNA. An almost identical value, namely 206 was obtained by our previous measurements[32]. These values are only slightly larger than the theoretical value of 197 for the B structure. Eisenberg and Cohen[29] have recently reported values of 196 and 166. These values were calculated from the data of Bram[28] and of Luzzati et al.[20,27,35] respectively. However, it has to be noted that the calculations of Eisenberg and Cohen are based on an electron density increment $(\delta\rho/\delta c_1)_\mu$ quite different from that used by us.

Eisenberg and Cohen calculated the electrondensity increment on the basis of a density increment of 0.457 as they had determined before pycnometric measurements[37] from. From this a value of 0.214 as electrondensity increment is obtained. On the other hand, our own measurements had led to a density increment of 0.439 from which the electrondensity increment of 0.204 was obtained. If we assume correctness of the density measurements themselves then the discrepancy between our results and those obtained by Eisenberg and Cohen must be caused by a different concentration standard. A similar conclusion is drawn by Eisenberg and Cohen[37]. As compared with the results obtained by these authors the concen-

trations of our solutions would have been overestimated and would really be about 4 % lower than assumed by us. Taking this into account the mass per unit length of pure NaDNA can be re-calculated from our data as 195. This value is now in excellent agreement with the B structure of DNA.

However, in the following we will refer again to the values reported in Table 4. A plot of these values is shown in fig. 19. The dashed line in the figure represents the dependance of M/Å upon r which is expected for mere binding of the actinomycin to the outside of the double helix. As can be seen from the figure the experimentally determined values are much lower and completely incompatible with this model. On the other hand they are in excellent agreement with the intercalation model. The relatively small increase of the mass per unit length by charging the DNA with actinomycin is understandable only by the assumption of an elongation of the helix, whereby the mass increase caused by the actinomycin would by partially compensated by a decrease of the mass per unit length of the DNA itself.

As we did before from the radii of gyration of the cross section we will now calculate the elongation l_A of the helix per bound actinomycin from the mass per unit length of the different samples. There holds

$$\frac{(M_D/r) + M_A}{(M_D/r)}$$

based on the data corrected according to Eisenberg and Cohen, namely $(M/\mathring{A})_o = 195$ and $(M/\mathring{A})_{0.16} = 207$. A similar value namely $l_A = 5.5 \pm 2.5$ Å was obtained when the calculation was performed with the data given in Table II for r = 0 and r = 0.05, but in this case the accuracy of the result is much lower.

However all values are in excellent agreement with the elongation of 4.4 Å as found for the system NaDNA-actinomine (see 4th Annual Report and[32]) by similar considerations and with the value of 4.5 Å derived from hydrodynamic measurements[7].

E) Conclusion

In the foregoing we have presented an extended study of the cross section of pure NaDNA and of NaDNA charged with different amounts of actinomycin.

The results obtained for pure NaDNA agree excellently with those found by previous measurements in our group[32] and those reported by Bram[28], Eisenberg and Cohen[29] and Bram and Beeman[36]. Our results agree also very well with the findings of Luzzati et al.[20,27,35], however there is a rather discrepancy in the mass per unit length[29]. Our results strongly favour the B structure of dissolved NaDNA.

Charging the DNA with actinomycin leads to a decrease of the radius of gyration of the cross section and to an increase of the mass per unit length much smaller than it is expected from the increase of total mass. Both findings are incompatible with any model of DNA-actinomycin interaction assuming mere binding of the actinomycin to the outside of the couble helix, but they strongly favour the validity of the intercalation model[7]. Our

results are interpreted by the assumption of a stretching of the double helix when charged with actinomycin. The elongation of the helix per bound actinomycin molecule is found to be 5 Å, which is almost identical with the values obtained by hydrodynamic measurements[7] and for the interaction of DNA and actinomine by former small angle X-ray experiments (4th Annual Report and [32]).

In the course of this study we made use of all new developments of experimental equipment and procedure. Some of them have been already described in previous Annual Reports. The computer program for smoothing the scattering curves which is presented in brief in this report is applicable mainly to simple scattering curves. However, it enabled us for the first time to perform the complete evaluation of the experimental data automatically in a single computer run.

II) DNA-, dependent - RNA - Polymerase

A) Materials and Methods

The enzyme DNA-dependent-RNA polymerase from E. coli was prepared following the improved method of Fuchs et al.[40]. The enzyme exists as dimer in solutions of low ionic strength and as monomer in solutions of high ionic strength. The sedimentation coefficient of the dimer has a value of about 24S, that of the monomer a value of 13S[40,41,42]. The disaggregation of the dimer into the monomer by increasing the ionic strength is a reversible process.

The holo-enzyme was studied in Tris-buffer at pH 7,4. The buffer contained also 0,01M Mg-acetate, 0,022M NH_4Cl, 0,001M mercaptoethanol and 0,0001M ethylenediaminetetraacetate. The density of the buffer was determined to be d = 0,999929 at 20°C (buffer A). By adding 0,5M KCl to this buffer a buffer with high ionic strength, in which the enzyme exists as monomer, was obtained.

The density of this buffer (buffer B) was 1,0232, the pH was 7,5. Besides the holo-enzyme as dimer and monomer a fragment of the enzyme - the so called core-enzyme - was studied, too. This core-enzyme is obtained from the holo-enzyme by chromatography on phosphorylcellulose. By this process the holo-enzyme is split into the core-enzyme and the initiation factor σ [43].

The homogenity was proved with all solutions by means of the analytical ultracentrifuge. Concentration series were made from the holo-enzyme dimer, the holo-enzyme monomer and the core-enzyme. In the following the results obtained from these three

samples are discussed in detail.

All small-angle measurements were carried out with an entrance slit of 150 μ (which corresponds to a maximum resolution of 550 Å Bragg spacing) and at a temperature of 5°C.

At each measuring point at least 10^5 pulses were registered and for each scattering curve 50 to 100 points (scattering angles) were measured.

B) Results

1. Holoenzyme - dimer

Two different preparations from the DNA-dependent RNA-polymerase were made and two concentration series were measured. The concentrations of the enzyme in the buffer A of low ionic strength (mentioned above), where the enzyme exists as dimer, were the following: 5,29; 5,48; 11,49; 12,1; 21,3; 52,6; 52,6 mg/ml. From each solution a scattering curve was measured and the corresponding blank curve of the buffer was subtracted with the help of a computer program. All curves were normalized to concentration one, that is, the I/c values were calculated.

a. Radius of gyration (R)

Fig. 20 gives the Guinier-plot of the slit-smeared scattering curves of the holo-enzyme dimer for the various concentrations.

At lower concentrations the R-values are nearly identical; at higher concentrations the usual concentration effects cause a decrease in intensity at small angles and therewith a

decrease in the slope of the straight line and in the R-value.

In Fig. 21 the slit-smeared R-values are plotted against the concentration of the enzyme. After extrapolation to zero concentration and elimination of the collimation effects the true values of the holo-enzyme dimer (24S) was found to be R = 95,0 Å (see Table 5). From the slit-smeared scattering curves all the data mentioned on the following pages are obtained, too.

b. Volume and molecular-weight

The individual V-values calculated with Q and I_o obtained for the two preparations are given in Table 5.

From the absolute intensity I_o/P_o, with $\bar{v}_1 = 0.535$ we found for the molecular weight of the holo-enzyme dimer

$$M = 9,95 \cdot 10^5 \pm 5\ \%.$$

The data calculated for the two different preparations of the enzyme are summarized in Table 5.

c) Shape

The scattering curve was measured very exactly over a large angle range in order to get as much information as possible on the shape of the molecule. The more maxima or minima are found in a scattering curve the more detailed information on the shape can be obtained. The scattering curve of the holo-enzyme dimer showed a shoulder and a maximum at larger angles.

A comparison of the experimental scattering curve with theoretical ones, calculated for simple triaxial bodies, showed that flat, hollow cylinders had similar curves. The comparison

was always carried out over a range of intensity of four orders of magnitude. It requires high accuracy to measure scattering curves, when the intensity has already dropped down to 1/10 000 of its original value.

Series of curves of flat hollow circular cylinders were calculated by a computer programme, whereby on the one hand the ratio height h of the cylinder to the outer diameter $2r_a$ was varied and on the other hand the ratio inner radius r_i to outer radius r_a of the cylinder, that is, the hollowness of the particle was varied. In Fig. 22 the experimental curve is compared with calculated curves of hollow cylinders, whereby the ratio $r_i : r_a$ is constant ($r_i/r_a = 0.2$), while the ratio $h : 2r_a$ is varied from 0,1; 0,2; 0,33; 0,4; 0,6; 0,8; to 1,0. Teh experimental curve agrees best with the hollow cylinder of the ratio $h : 2r_a = 0,4$. In Fig. 23 the experimental scattering curve is compared with theoretical curves of circular hollow cylinders; the ratio $h/2r_a$ is the same for all cylinders namely 0,4. Varied is only the ratio $r_i:r_a$; it has the values 0 (full cylinder), 0,1; 0,2; 0,3; 0,4 and 0,5. All theoretical curves are calculated for bodies which have the same radius of gyration (R = 95,0 Å) as was experimentally found for the holo-enzyme dimer. It is clearly seen that the shoulder in the scattering curve is the more pronounced the greater the ratio r_i/r_a and with it the hollowness of the body.

The best agreement is found for a ratio $h:2r_a = 0,4$ and r_i/r_a about 0,2. Now in this range the ratio r_i/r_a was varied in smaller steps and theoretical scattering curves were calculated, which had ratios r_i/r_a of 0,1; 0,15; 0,2; 0,25; 0,3.

In Fig. 24 the experimental curve is compared in the same way with these curves.

Here it is seen too, that the experimental curves fit best to a hollow cylinder with the ratios $h/2r_a = 0,4$ and $r_i/r_a = 0,2$. The curve of the holo-enzyme dimer does not only agree in its whole course but also in the height and position of the shoulder and the maximum. We can say that the holo enzyme dimer is equivalent in scattering to this flat, hollow cylinder.

From the axial ratio of this cylinder and the experimentally found R-value of 95,0 Å the following dimensions can be calculated for the cylinder: height h = 100 Å, outer diameter $2r_a = 250$ Å, inner diameter $2r_i = 50$ Å.

2. Holo-Enzyme Monomer

Measurements with the ultracentrifuge seemed to indicate that the holo-enzyme dimer (24S) splits into two identical monomers (13S), when the ionic strength of the buffer is increased.

To study this monomer, too, the holo-enzyme dimer solution (buffer A) was dialyzed against a buffer with high ionic strength (buffer B). A series of various concentrations was measured; the concentrations of the enzyme were: 5,43; 10,71; 21,20; 34,20 and 67,60 mg/ml.

The scattering curves were evaluated in the same way as described for the holo-enzyme dimer.

In Fig. 25 the inner portions of the scattering curves are plotted according to Guinier. The straight-lined course is not so pronounced as with the holo-enzyme dimer (see Fig. 20) or

with the core-enzyme (Fig. 28). This indicates already that the solutions of the monomer are not quite homodisperse. After elimination of the collimation effect the curve shown in Fig.26 (curve 2) is obtained. Now it is clearly seen that the solution of the monomer is polydisperse, no straight line is obtained in the Guinier plot as is with curve 1 and curve 3, which correspond to the holo-enzyme dimer and to the core-enzyme.

For the radius of gyration an average value of

$$R \approx 51 \text{ Å}$$

is obtained and for the molecular-weight an average value of

$$M \approx 3{,}3 \cdot 10^5$$

Both values are definitely too low assuming that the monomer is really the half of the dimer. The reason for these low values is the splitting of the monomer into two further subunits called the core-enzyme and the σ- factor, as is shown in the section "discussion" in detail. In this section the course of the scattering curve, which the holo-enzyme has in solution of high ionic strength (Fig. 27) is discussed, too.

3. Core-Enzyme

By chromatography on phosphorylcellulose the holo-enzyme monomer can be split into two subunits the so called "core-enzyme" and the " σ -factor".

A homogeneous solution of the core-enzyme was studied in buffer B. Two different preparations of the enzyme were made and two series of concentrations were measured. Individually the solutions of the core-enzyme had the following concen-

trations: 3,97; 6,85; 9,64; 11,0; 14,7; 19,32; 21,9 and 43,9 mg/ml.

The X-ray small angle measurements were carried out in the same way as described for the holo-enzyme dimer.

a) Radius of gyration

In Fig. 28 the inner portions of the slit-smeared scattering curves of the various concentrations are plotted according to Guinier and the apparent radii of gyration (R) are determined from the slope of the straight lines. The concentrations and the R-values obtained are given in the figure.

In Fig. 21 the R-values are plotted against the concentration of the core-enzyme (lower curve); the extrapolation to zero concentration gives a value $R_{c \rightarrow o} = 57,5$ Å. After elimination of the concentration effects the true radius of gyration was found to be

$$R = 60,5 \text{ Å}.$$

The individual data of the two preparations are given in Tab.5.

b) Volume and molecular-weight

With Q and I_o a value of

$$V = 9,7 \cdot 10^5 \pm 5 \% \text{ Å}^3$$

was calculated for the volume of the core-enzyme.

To determine the molecular-weight the partial specific volume of the core-enzyme in buffer B was measured at 5°C; a $\bar{v}$-value of 0.732 was obtained. With this value the molecular-weight M was calculated as

$$M = 3,8 \cdot 10^5.$$

Compare also the data for the individual preparations in Table 5.

c) Shape

In Fig. 29 the scattering curve of the core-enzyme is shown in log-log plot. A comparison with theoretical scattering curves of various triaxial bodies showed that the overall shape of the core-enzyme corresponds to an axial ratio of about 1:1:2. But neither an ellipsoid nor a cylinder coincides completely with the experimental curve and especially with the height and position of the subsidiary maximum present in this curve. So we have to assume that the core-enzyme has a more complicated shape and cannot be described very well by a simple triaxial body.

C) Discussion

If we summarize the results obtained we get the following picture. The molecular-weights found for the holo-enzyme dimer and the core-enzyme agree in all essentials with the values, which other authors[40,44,45,46,47,48] obtained by ultra-centrifuge measurements and calculated from the molecular weight of the known subunits of the enzyme[49]. The results are summarized in Table 6.

The authors generally used in their calculations of the M-value for the partial specific volume a value which was calculated only from the amino acid composition of the enzyme. Since the $\bar{v}$-value of a protein essentially depends on the

solvent, especially on the ionic strength of the buffer used, the use of the $\bar{v}$-value, calculated only from the amino acid composition, is a rough approximation. We determined the $\bar{v}$-value of the enzyme in each case in the same buffer used in the small angle measurements in order to determine the molecular-weight as exactly as possible.

Ultracentrifuge investigations had shown that at a high ionic strength the holo-enzyme dimer splits into two monomers, which sediment as an apparently uniform peak with a constant 12,8S - 13S.

Our small angle X-ray measurements showed that it is not the pure monomer which is present at high ionic strength but a mixture of core-enzyme and σ-factor. Obviously the monomer splits at higher ionic strength immediately into these two subunits. This result can be seen from Fig. 26 . The core-enzyme and the apparent monomer were investigated under completely identical conditions (same capillary, same buffer, same electron density difference, etc.) and the curves obtained were normalized to the same concentration c. Under these conditions the scattering intensity at zero angle I_o depends only on the molecular-weight M of the particles in solution. The monomer would have to have half the M of the dimer, that is to say, about 490 000. Since the core-enzyme has a M of 380 000, the I_o-value for the monomer would have to be roughly 20 % higher. But as it can be seen from curves 2 and 3 in Fig. 26 the I_o-value for the monomer is, however, 15 % lower. This fact can only be explained if one assumes that almost all monomer particles have split into the core-enzyme and the σ-factor.

For the mixture of these two subunits a mean molecular-weight of 330 000 is calculated, which agrees with the experimentally found value.

The M-values found by ultracentrifuge for the monomer (see Table 6) are also definitely too low; they are very similar to the molecular-weight found for the core-enzyme. But the monomer consists of the core-enzyme and the -factor and the molecular-weight of the latter was determined to be about 90 000. So it is not to be understood, why - with the ultracentrifuge measurements - for the core-enzyme and the monomer nearly the same values are found. Since our measurements show clearly, that the monomer splits into the core-enzyme and -factor it must be assumed that a similar splitting takes place when the monomer is studied with ultracentrifuge and this may be the reason, while the M-value of the monomer was found too low.

D) Conclusions

If we assume that the whole mass of the holo-enzyme dimer is concentrated in a sphere, this sphere would have a radius of gyration of only 48 Å. The true radius of gyration is much greater, it has a value of 95 Å. This result already shows that the molecule must be very extended.

Comparison with various theoretical curves indicated that the enzyme is equivalent in scattering to a flat hollow cylinder with the dimensions: height h = 100 Å, outer diameter $2r_a$ = 250 Å and inner diameter $2r_i$ = 50 Å.

We must assume that this cylinder is not filled homogeneously with mass because its volume ($V = 4{,}7 \cdot 10^6$ Å^3) is clearly higher than the experimentally found volume of $3{,}5 \cdot 10^6$ Å^3.

First electronmicrographs seem to confirm our results, since sometimes a ring composed of subunits is seen, which can be interpreted as the view on the top of our hollow cylinder; and this ring seemed to be composed of subunits. But up to now these micrographs are not very clear and the dimensions obtained for the enzyme therefrom are much to small.

Our model of a flat hollow cylinder is to be harmonized with the function of the DNA - dependent RNA-Polymerase. A possible model for this enzyme, already suggested by Zillig[48], is the following. The enzyme runs along the DNA like a hollow cylinder is moved over a strand. While the enzyme moves along the DNA-strand it separates the codogenic strand from the non-codogenic strand at a site. Now the genetic code of the codogenic strand of the DNA can be read and the RNA is synthetized. While the enzyme moves along the DNA the already synthetized part of RNA strand is displaced from the codogenic strand and the native double strand of DNA is formed back.

Of course there are a lot of questions, which the studies we want to perform in the near future may answer. Some of them are the following:

Is it possible to find conditions under which the holo-enzyme monomer is stable, so that we can clarify whether this monomer is a half cylinder and whether the holo-enzyme dimer is built up on the DNA-strand from the two halves?

Does the enzyme, when it is fixed on the DNA-strand, really open the two single strands (codogenic and non-codogenic strand) by splitting the hydrogen-bonds between the base-pairs?

Experimental Method

The experimental method which we use for measurement of small-angle X-ray scattering has been described in various summarizing presentations[50-56]. The most important things have likewise been said in yearly reports 1-4. However, we intend here to give a short summary of the essential points and to make some supplementary remarks:

1) Climate

It is necessary to condition the room to a constant temperature of $\pm$ 1°C and a relative humidity of $\pm$ 5%.

2) Cooling water

We use a closed cooling water circulation with a temperature regulation of $\pm$ 0.5°C. This measure has at the same time the advantage that no sedimentation forms in the X-ray tube to hinder the effect of cooling and the flow of water.

3) X-ray tube

The process of desmearing (see point 6) is always unequivocally workable, when the primary beam shows a constant intensity in the registration plane along a sufficiently long line. This goal can be achieved, when the diameter of the window of the X-ray tube in larger than the length of the focus[57,53,54].

Philips has, with a view to this demand developed at our suggestion an X-ray tube in which the size of the focus is 12x2 mm^2, the window diameter 16 mm. Siemens has built

a similiar tube with the focus 7x2·5 mm^2 and the window diameter 10 mm.

4) Small-angle camera and accessories

The small-angle camera developed and used by us is practically free from parasitic scattering and has already been described in detail[58,59,60]. For the movement of the counting-tube a step-scanning device, also developed by us, was used[61]. Detailed description is given in report 1.

5) Impulse-counting device and monochromatizing

For impulse-counting we made use of manufactured apparatuses. They contained an impulse height discriminator which was adjusted to the CuKα-line. This measure suffices to suppress adequately the continuous radiation. For the elimination of the β-line, which is not possible in this way, a mathematical procedure was developed and described in detail in the 2. report[62].

6) Desmearing

The line-shaped form of the primary beam-cross-section influences the shape of the scattering curve. This influence must be eliminated. We call the process desmearing. It is effected according to well-known procedures[63,64,65]. For the practical execution we make use of a computer programme prepared in our working group [66,67]. The experimental measured intensity is designated as $\tilde{I}$, the value after desmearing as I.

7) Evaluation

Attention is invited to summarizing descriptions[50-56].

Particulate scattering is the scattering curve(=plotting of the scattered intensity I against the scattering angle 2θ[+]) of an "infinitely" dilute homodisperse system, usually a solution, and it characterizes the individual particles according to mass, size and shape. In order to obtain the particulate scattering the scattering curves for a series of concentrations should be measured and all curves should be standardized to the unit of concentration c (e.g. 1 mg/ml). A series of curves of this kind makes possible the extrapolation to zero concentration when measurements were made to sufficiently small concentrations (a few mg/ml). Use can be made of the natural plot I/c against 2θ or of the Guinier plot log I/c against $(2\theta)^2$.

From the particulate scattering a number of important quantities can be derived:

a) Radius of gyration. In the Guinier plot each particulate scattering approximates to a straight line at very small angles ($2\theta \rightarrow 0$. From its slope ($tg\alpha$) the radius of gyration R is obtained with λ = 1.54 Å (CuKα-line) according to the equation of Guinier[50]

$$R = 0{\cdot}644 \sqrt{(tg\alpha)_o}$$

+) In the presentation of the scattering curve the distance m of the measuring point in the registering plane from the centre of the primary beam (=cross-section) is often taken as abscissa. With good approximation the relation $m/a = 2\theta$ is valid, whereby a = distance sample-registering plane.

R is the root mean square of the distances of the electrons from the electronic centre of gravity of the particle and is thus a measure for the spatial extent of a particle.One can also extrapolate to zero concentration the "apparent" radius of gyration which is determined at various concentrations.

Studies of the radius of gyration may be interesting when examining changes in shape. As an examply we have discussed the temperature dependency of phenylalanin specific t-ribonucleid acid.

b) Shape The shape of a particle is characterized by the deviation of its scattering curve from the Guinier straight line; the more convex the curve is against the abscissa the more anisotropic is the shape. Mostly the determination of the shape is made in the plot log I against log 2θ .

Inclusion of the subsidiary maxima is of great importance for determination of the shape.

c) Molecular-weight The small-angle X-ray scattering method is also a procedure for "weighing" in colloidal dimensions. The determination of the molecular-weight is made according to the following equation[68,53]

$$M = \frac{I_o}{P_o} \cdot \frac{21^{\cdot}0.a^2}{(z_1 - \bar{v}_1 \varrho_2)^2.d.c} \qquad (2)$$

Here I_o is the scattering intensity extrapolated to zero concentration, d [cm] is the thickness of the sample, c [g/ml] the concentration and P_o the primary intensity. It was possible to solve the problem of the measurement of P_o by the development of calibration samples in the

form of polyethylen platelets[69] which in their turn were calibrated according to a procedure developed at our Institute[70]. $\bar{v}_1$ is the partial specific volume of the solute substance which is obtained from the density of its solution. For this purpose a precision instrument was developed for extremely exact determination of the density of liquids (to six digits)[71], which has been described in the 2. report. z_1 is the number of molelectrons per g of the solute substance, ϱ_2 is the electron density of the solvent. The accuracy of the molecular-weight determination according to this procedure is not excelled by any other method.

d) Volume The volume of the solute particles can be calculated as follows[72]:

$$V = 0{\cdot}291\ I_o/Q\ \text{Å}^3 \qquad Q = \int_o^\infty I(2\Theta)^2\, d\,(2\Theta) \quad (3a)$$

or

$$V = 0{\cdot}582\ I_o/\tilde{Q}\ \text{Å}^3 \quad \tilde{Q} = \int_o^\infty \tilde{I}\,(2\Theta)\, d\,(2\Theta) \quad (3b)$$

The quantity Q or $\tilde{Q}$ we designate as invariant.

e) Cross-section factor With elongated particles the scattering curve I can be split into two factors[73].

$$I = I_q \cdot \frac{1}{(2\Theta)} \quad (4a)$$

The first factor I_q derives from dimensions and shape of the cross-section and is called the cross-section factor. The second factor $\frac{1}{2\Theta}$ refers to the lenght of the particle. Its meaning is understood from the indication that a gas of infinitely long and infinitely thin particles would have

a scattering curve $\frac{1}{2\Theta}$. When these particles have a finite cross-section the cross-section factor I_q is added by multiplication. It can be found according to equation(4a) as follows:

$$I_q = I.(2\Theta) \qquad (4b)$$

From this cross-section factor I_q analogous information regarding the cross-section can be obtained just as from the scattering intensity I regarding the whole particle:

α) From the slope of the Guinier plot of the cross-section factor log I_q against $(2\Theta)^2$ at small angles $(2\Theta \to 0)$ the radius of gyration of the cross-section is obtained according to[73]:

$$R_q = 0.526 \sqrt{(tg\alpha)_o} \text{ Å} \qquad (5)$$

β) Analogous to (2) we can calculate from the absolute value of the intensity at zero angle of the cross-section factor $(I.2\Theta)_o$ the mass per unit lenght M/1Å of the cross-section[74,53]:

$$M/\text{Å} = \frac{(I_q)_o}{P_o} \quad \frac{27{\cdot}3\ a^2}{(z_1 - \bar{v}_1 \rho_2)^2 . d . c} \qquad (6)$$

This unique possibility of the small-angle X-ray scattering method allows the unit lenght to be "weighed", independently of the size of the particle.

γ) Analogous to (3) we can determine from the cross-section factor the area A of the cross-section[72].

$$A = 0{\cdot}378\ (I.2\Theta)_o / Q\ \text{Å}^2 \qquad (7)$$

δ) From the form of the cross-section factor the shape

of the cross-section can be obtained analogous to b).When the particles are not infinitely long the cross-section factors deviate downwards from the Guinier straight line at small angles. This loss of intensity at small angles is caused by the lack of great distances with particles which are not infinitely long. This is evident, because according to the universally valid reciprocity law of optics great distances scatter to small angles.

f) Thickness factor With lamellar particles, too, the scattering curve can be split into two factors[73]:

$$I = I_t \cdot \frac{1}{(2\theta)^2} \qquad (8a)$$

The first factor I_t derives from the thickness and is called thickness factor. The second factor $\frac{1}{(2\theta)^2}$ refers to the area extension of the particle. Its meaning is understood from the indication that a gas of particles with infinitely large and infinitely thin areas would give a scattering curve $\frac{1}{(2\theta)^2}$.

If these platelets have a finite thickness, the thickness factor is added by multiplication. It is calculable according to (8a) as follows).

$$I_t = I.(2\Theta)^2 \qquad (8b)$$

From this thickness factor analogous information can be deduced as from the cross-section factor.

α) From the Guinier plot of the thickness factor, i.e. log I_t against $(2\Theta)^2$ one obtains from the slope at small angle $(2\Theta \rightarrow 0)$ the radius of gyration of the thickness R_t

and the thickness I itself as follows:

$$R_t = 0.372 \sqrt{(tg\alpha)_o}\,\text{Å};\quad t = R_t \times \sqrt{12}\,\text{Å} \qquad (9)$$

β) Similarly to (2) and (6) the mass per unit of area can be calculated from the absolute value of the intensity at zero angle of the thickness factor $\left[I.(2\Theta)^2\right]_o/P_o$. This possibility of small-angle X-ray scattering, which is also unique, allows the unit of area to be weighed, independently of the size of the particle[68,53].

g) Persistence lenght The study of the coiled filamentary molecules in solution renders possible, in the same way as that discussed above, the determination of R, R_q, M, M/Å. Such solutions, however, are usually not homodisperse; the figures obtained represent in this case average values.

A further characteristic of the solute filamentary molecule is the persistence length. It corresponds exactly to half the W.Kuhn statistical filamentary element and is a measure for the degree of coiling. In the plot of $I.(2\Theta)^2$ against (2Θ) one obtains a curve composed of two branches of different slopes. By the extrapolation of the two branches towards the transition zone, we get a fairly definite transition point. From its abscissa $(2\Theta)^+$ the persistence length a^+ is calculated as follows[75,76]:

$$a^+ = 2x2{\cdot}3\,\frac{\lambda}{4\pi}\cdot\frac{1}{(2\Theta)^+} \qquad (10)$$

The branch to the left of the transition point differs in its slope the more from the branch to the right of the transition point the greater the length of the molecule is as compared to the persistence length.

Table 1

Apparent radii of gyration ($\tilde{R}$) of $tRNA^{Phe}_{yeast}$ at various concentrations (c) of tRNA and various counter ions.

a) $Spermidin^{++}$-tRNA

Fig.27 Nr.	c [mg/ml]	$\tilde{R}$ [Å]
1	2.5	22.4
2	5.0	22.2
3	7.5	21.8
4	10	21.4
5	15	21.2
6	20	21.4
	$c \rightarrow o$	22.7

f) $Spermidin^{++}$-tRNA (+Spermidin . HCl)

Fig.29 Nr.	c [mg/ml]	$\tilde{R}$ [Å]
1	2.5	25.6
2	5.0	26.0
3	7.5	25.6
4	10	(26.0)
5	20	(26.0)
	$c \rightarrow o$	25.6

Table 2

Calculated molecular weights M and experimentally found radii of gyration R of $tRNA^{Phe}_{yeast}$ with various counter ions.

1	2	3					4
ion	atomic weight of the ions	M (tRNA)	+	weight of the counter ions			R [Å]
-		24890					-
Li^+	6.9	24890	+	534	=	25424	23.6
Cs^+	133	24890	+	10230	=	35120	26.2
Ba^{++}	137	24890	+	5286	=	30176	26.3
K^+	39	24890	+	3011	=	27901	
Mg^{++}	24	24890	+	935	=	25825	
$Mg^{++} + K^+$	24 - 39					(25800 - 27900)	24.4

Table 3

Radii of gyration of the cross section R_c of sonicated NaDNA in dependence upon r, the number of actinomycin molecules bound per base pair

r	c (mg/ml)	R_c (Å)
0	8.7	8.64
	8.7	8.69
	8.7	8.62
	4.35	8.84
	averaged	8.7
0.025	8.7	8.57
0.05	8.7	8.59
	8.7	8.54
	8.7	8.43
	4.35	8.40
	averaged	8.5
0.1	8.7	8.32
0.16	8.7	8.05
	8.7	8.19
	4.35	8.13
	averaged	8.1

Table 4

Mass per unit length M/Å of sonicated NaDNA in dependence upon the amount of bound actinomycin

r	M/Å
0	207 ± 5
0.05	209 ± 6
0.16	217 ± 3

Table 5

Data obtained for DNA-dependent RNA-polymerase of two different preparation.

	1.Preparation (June 1970)	2.Preparation (March 1971)
Holo-enzyme (dimer) (low ionic strength)	$M=9,90.10^5$ $V=3,50.10^6 Å^3$ $R=95,0 Å$ $\bar{v}(5^oC)=0,735$	$M=9,98.10^5$ $V=3,53.10^6$ $R=94,5 Å$ $\bar{v}(5^oC)=0,735$
Holo-enzyme (high ionic strength)	polydisperse	$\bar{M}=3,3.10^5 \pm 10\%$ $\bar{R}=51 Å \pm 5\%$ $\bar{v}(5^oC)=0,737$
Core-enzyme	$M=3,74.10^5$ $V=1,0.10^6 Å^3$ $R=60,1 Å$ $\bar{v}(5^oC)=0,732$	$M=3,85.10^5$ $V=0,93.10^6 Å^3$ $R=60,5 Å$ $\bar{v}(5^oC)=0,732$

Table 6

Molecular-weights (M) of DNA dependent RNA-polymerase obtained by ultracentrifuge and by small angle measurements: ($\bar{v}$ = partial specific volume used for the calculations).

			Holo-enzyme			
No.	Author	Method	dimer M x 10^{-5}	monomer M x 10^{-5}	Core enzyme M x 10^{-5}	$\bar{v}$
1	Richardson (1966) [41]	ultracentrifuge	8,8 ± 1,6	4,4 ± 0,8		0,73+
2	Maitra and Hurwitz (1967) [44]	-"-		3,7		0,73+
3	Priess and Zillig (1967) [45]	-"-		3,6 ± 0,4		0,74+
4	Berg and Chamberlin (1970) [47]	-"-		3,9 ± 0,1	3,6	0,72+
5	Pilz, Kratky and Rabussay	small angle	9,95 ± 0,5	-	3,8 ± 0,15	0,732++ (Core-enzyme) 0,735++ (Holo-enzyme)
6	Berg and Chamberlin (1970) [47]	calculated from the subunits	9,26 ± 10%		3,77 ± 10%	
7	Burgess (1969) [46]	-"-	9,86 ± 1,0		3,98 ± 10%	
8	Zillig et al. (1969) [48]	-"-	9,4 ± 10%		3,85 ± 10%	

+) calculated from amino acid composition

++) measured in the corresponding buffer

Literatur

1) W.Kersten, H.Kersten and H.M.Rauen, Nature London 187, 60 (1960).

2) E.Harbers and W.Müller, Biochem.biophysic.Res.Commun. 7, 107 (1962).

3) G.Hartmann and U.Coy, Angew.Chem. 74, 501 (1962).

4) J.Hurwitz, J.J.Furth, M.Malamy and M.Alexander, Proc.nat.Acad. Sci. 48, 122 (1962).

5) I.H.Goldberg, M.Rabinowitz and E.Reich, Proc.nat.Acad.Sci. 48, 2094 (1962).

6) L.D.Hamilton, W.Fuller and E.Reich, Nature London 198,538 (1963).

7) W.Müller D.M.Crothers, J.molecular Biol. 35, 251 (1968).

8) R.W.Wells, Science N.Y. 165, 75 (1969).

9) J.A.Lake and W.W.Beeman, J.Mol.Biol 31, 115 (1968).

10) W.R.Krigbaum and R.W.Godwin, Science, 154, 423 (1966).

11) J.Ninio, A.Favre and M.Yaniv, Nature (London), 223, 1333 (1969).

12) S.Heine, O.Kratky, G.Porod and P.J.Schmitz, Makromol.Chem. 44-46, 682 (1961).

13) O.Kratky and G.Porod, Rec.Trav.Chim.Pays-Bas. 68, 1106 (1949).

14) G.Porod, J.Polymer Sci. 10, 157 (1953).

15) P.G.Connors, M.Labanauskas and W.W.Beeman, Science 166, 1528 (1969).

16) J.Ninio, A.Favre and M.Yaniv, Nature (London), 223, 1333 (1969).

17) G.Melcher, FEBS Letters, 3, 185 (1969).

18) F.Cramer, H.Doepner, F.von der Haar, E.Schlimme and H.Seidel, Proc.Nat.Acad.Sci.U.S.A., 61, 1348 (1968).

19) M.Levitt, Nature (London), 244, 759 (1969).

20) V.Luzzati, A.Nicolaieff and F.Masson, J.Mol.Biol. 3, 185 (1961).

21) S.N.Timasheff, J.Witz and V.Luzzati, Biophys.J., 1, 525 (1961).

22) R.Rolfe and M.Meselson, Proc.Nat.Acad.Sci.U.S.A. 45, 1039 (1959).

23) R.G.Kirste and B.H.Stuhrmann, Z.Physik.Chem., Neue Folge 56, 5/6 (1967).

24) F.Cramer, F.von der Haar, K.C.Holmes, W.Saenger, E.Schlimme and G.E.Schulz, J.Mol.Biol., in press.

25) D.D.Henley, T.Lindahl and J.R.Fresco, Proc.Nat.Acad.Sci.U.S.A. 55, 191 (1966).

26) F.Oosawa, Biopolymers, 9, 677 (1970).

27) V.Luzzati, F.Masson, A.Mathis and P.Saludjian, Biopolymers, 5, 491 (1967).

28) S.Bram, Ph.D. Thesis, University of Wisconsin 1968.

29) H.Eisenberg and G.J.Cohen, J.Mol.Biol. 37, 355 (1968).

30) R.W.Holley, J.Apgar, G.A.Everett, J.T.Madison, M.Marquisee, S.H.Merill, J.R.Penswick and A.Zamir, Science 147, 1462 (1965).

31) L.S.Lerman. J.molecular Biol. 3, 18 (1961).

32) H.Wawra, W.Müller and O.Kratky, Makrom.Chem. 139, 83 (1970).

33) S.Heine and J.Roppert, Acta Physica Austriaca 15, 148 (1962); S.Heine, Acta Physica Austriaca 16, 144 (1963).

34) P.Zipper, Acta Physica Austriaca 30, 143 (1969).

35) V.Luzzati, F.Mason and L.S.Lerman, J.Mol.Biol. 3, 634 (1961).

36) S.Bram and W.W.Beeman, J.Mol.Biol. 55, 311 (1971).

37) G.Cohen and H.Eisenberg, Biopolymers 6, 1077 (1968).

38) W.Müller and I.Emme, Z.Naturfschg. 20b, 835 (1965).

39) R.Langridge, D.A.Marvin, W.E.Seeds, H.R.Wilson, C.W.Hooper, M. H.F.Wilkins and L.D.Hamilton, J.Mol.Biol. 2, 38 (1960).

40) E.Fuchs, W.Zillig, P.H.Hofschneider and A.Preuss, J.Mol.Biol. 10, 546 (1964).

41) J.P.Richardson, Proc.Natl.Acad.Sci.US. 55, 1616 (1966).

42) K.E.van Holde and R.L.Baldwin, J.Phys.Chem. 62, 734 (1958).

43) R.R.Burgess, A.A.Travers, J.J.Dunn and E.K.F.Bautz, Nature 221, 43 (1969).

44) U.Maitra and J.Hurwitz, J.Biol.Chem. 242, 4897 (1967).

45) H.Priess and W.Zillig, Biochim.Biophys. Acta 140, 540 (1967).

46) R.R.Burgess, J.Biol.Chem. 244, 6168 (1969).

47) D.Berg and M.Chamberlin, in press.

48) W.Zillig, E.Fuschs, G.Walter, R.L.Millette and H.Priess in: The Biochemistry of Virus Replication, p. 37, Universitetsforlaget, Oslo, 1968.

49) W.Seifert and W.Zillig "20. Colloquium der Gesellschaft für Biologische Chemie" (1969) Mosbach/Baden. Springer-Verlag p.32.

50) A.Guinier and G.Fournet, Small Angle Scattering of X-Rays, J. Wiley Sons Inc., New York and Chapmann & Hall, London 1955.

51) W.Beeman, P.Kaesberg, J.W.Anderegg and M.B.Webb, Size of Particles and Lattice Defects, in: Handbuch der Physik, Bd. 32, ed. by S.Flügge, Springer Verlag 1957.

52) O.Kratky, Diffuse Röntgenkleinwinkelstreuung, Bestimmung von Größe und Gestalt von Kolloidteilchen und Makromolekülen, Angew. Chem., 72, 467 (1960).

53) O.Kratky, X-Ray Small Angle Scattering with Substances of Biological Interest in Diluted Solution, in: Progress in Biophysics, Vol.13, Pergamon Press, Oxford, London, New York, Paris 1963.

54) O.Kratky, Proceedings of the Conference held at Syracuse University, June 1965 on "Small-Angle X-Ray Scattering", ed. by H.Brumberger, Gordon and Breach, Science Publ. New York, London, Paris.

55) O.Kratky, Possibilities of X-ray small-angle analysis in the investigation of dissolved and solid high polymer substances, Pure and Appl.Chem. 12, 483 (1966).

56) L.E.Alexander, X-Ray Diffraction Methods in Polymer Science, Wiley-Interscience, John Wiley & Sons, Inc., New York-London-Sydney-Toronto 1969, p. 280-353.

57) O.Kratky, G.Porod and Z.Skala, Acta Physica Austriaca 13, 76 (1960).

58) O.Kratky, Z.Elektrochem. 58, 49 (1954).

59) O.Kratky, Z.Elektrochem. 62, 66 (1958).

60) O.Kratky and Z.Skala, Z.Elektrochem., 62, 73 (1958).

61) H.Leopold, Z.angew.Physik, 25, 81 (1968).

62) P.Zipper, Acta Physica Austriaca, 30, 143 (1969).

63) A.Guinier and G.Fournet, J.Phys.Rad. 8, 345 (1947).

64) O.Kratky, G.Porod and L.Kahovec, Z.Elektrochem., 55, 53 (1950).

65) O.Kratky, G.Porod and Z.Skala, Acta Physica Austriaca, 13, 76 (1960).

66) S.Heine and J.Roppert, Acta Physica Austriaca, 15, 148 (1962).

67) S.Heine, Acta Physica Austriaca, 16, 144 (1963).

68) O.Kratky, G.Porod and L.Kahovec, Z.Elektrochem. 55, 53 (1950), O.Kratky, Z.analyt. Chem. 201, 161 (1964).

69) O.Kratky, I.Pilz and P.J.Schmitz, J.Colloid Interface Sci. 21, 24 (1966),
I.Pilz and O.Kratky, J.Colloid Interface Sci. 24, 211 (1967),
I.Pilz, J.Colloid Interface Sci. 30, 140 (1969).

70) O.Kratky, Makrom.Chem. 35A, 12 (1960),
O.Kratky and H.Wawra, Mh.Chem. 94, 981 (1963).

71) O.Kratky, H.Leopold and H.Stabinger, Z.angew.Physik 27, 273 (1969).

72) G.Porod, Kolloid-Z. 124, 83 (1951); 125, 51 (1952).

73) O.Kratky and G.Porod, Acta Physica Austriaca 2, 133 (1948), G.Porod, Acta Physica Austriaca 2, 255 (1948).

74) O.Kratky and G.Porod, in: Die Physik der Hochpolymeren, Vol.II, ed by H.A.Stuart, Springer-Verlag, Berlin 1955, p.515.

75) O.Kratky and G.Porod, Rec.Trav.Chim.Pays-Bas 68, 1106 (1949), G.Porod, J.Polymer Sci. 10, 157 (1953).

76) S.Heine, O.Kratky and J.Roppert, Makrom.Chem. 56, 150 (1962).

Legends to the Figures

Fig. 1 Middle portions of the scattering curves of a concentrations series of Na-DNS in 0,1 m NaCl, pH7.

Fig. 2 Inner portion of the scattering curve (with collimation error) of Na-DNS in 0,30 m NaCl pH7. The curve obtained by extrapolation to zero concentration of the scattering curve shape is designated with c = o.

Fig. 3 Scattering curve corrected for collimation error, obtained from the curve marked with c = o in Fig.2.

Fig. 4 Guinier-plot (log.IR versus θ^2) of the inner portion of the scattering curve (corrected for collimation error) of Na-DNS, and of the DNS-A complex. Ordinates have been shifted.

Fig. 5 Guinier-plot of the cross section factor (log.($I\theta$)) versus θ^2), for both Na-DNS and DNS-A complex.

Fig. 6 Measured and desmeared cross-section curves of the pure DNA for all measured concentrations. The outer portion is continued inward as Gauss curve (broken lines).

Fig. 7 Radial electron density distribution around the axes of the DNA-molecule.

Fig. 8 Scattering curves of t-RNA^{Phe}_{yeast} in 0.05 M tris-buffer, pH 7.5 at different temperatures. $\tilde{I}$ is the intensity in imp/sec, c the concentration in mg/ml, the scattering angle 2θ is given in radians and the corresponding Bragg spacing in Å. The concentrations of the solution

were 1.5 mg/ml (Δ), 3.03 mg/ml (o), 5.88 mg/ml (x), 10.6 mg/ml (o), 11.3 mg/ml (■) and 20.9 mg/ml (+).

Fig. 9 Guinier plot of the inner portion of the scattering curves in fig. 1. The concentrations of the solutions are the same as in fig. 1. The full lines correspond to the scattering curves extrapolated to the concentration zero. The radii of gyration are given. The curves and the R-values are not corrected for the collimation-effect.

Fig. 10 Radii of gyration R, depending on concentration and temperature.

Fig. 11 Experimental scattering curve (o) of t-RNA$^{Phe}_{yeast}$ at 17°C compared with the theoretical scattering curves of rotational cylinders of various axial ratios v (closed lines), with the theoretical curve of the model formed from three ellipsoids (Δ) and with a curve (x) calculated approximately by the Debye-formula from the model described in[1].

Fig. 12 Cross-section factors of t-RNA$^{Phe}_{yeast}$ at 17°C.
Curve 1: in 0.05 M tris-buffer and 10^{-2} M Mg^{++}
R_{q1} = 11.0 Å, R_{q2} = 9.5 Å.
Curve 2: in 0.05 M tris buffer
R_{q1} = 11.0 Å, R_{q2} = 9.1 Å.
Curve 3: cross section curve of the model in fig. 7.
R_{q1} = 10.9 Å, R_{q2} = 9.3 Å.

Fig. 13 Melting curve of t-RNA$^{Phe}_{yeast}$ and dependence of the radius of gyration from the temperature.

Fig. 14 Experimental scattering curve of t-RNA^{Phe}_{yeast} at 70°C (curve 2) and theoretical scattering curve of a coil calculated according to the Monte-Carlo-method for 18 lengths of persistence (curve 1).

Fig. 15 Apparent radii of gyration $\tilde{R}$ of $tRNA^{Phe}$, summarized in table 1, plotted against the concentration c of $tRNA^{Phe}$.

Fig. 16 Slit-corrected radii of gyration R of $tRNA^{Phe}$ plotted against the atomic weight of the counter ions used.

Fig. 17 Scattering curves of sonicated NaDNA charged with different amounts of actinomycin C_3. Curves 1 - 4 : r = 0; 5 : r = 0.025; 6 - 9 : r = 0.05; 10 : r = 0.1; 11 - 13 : r = 0.16. The concentration of NaDNA is 8.7 mg/ml for curves 1,2,3,5,6,7,8,10,11,12 and 4,35 mg/ml for curves 4,9,13 respectively.

Fig. 18 Dependence of the radius of gyration of the cross section R_c of sonicated NaDNA upon the amount of bound actinomycin. (r = number of actinomycin molecules bound per base pair).

Fig. 19 Dependence of the mass per unit length of sonicated NaDNA upon the amount of bound actinomycin. The dashed line represents the mass increase expected for a model which assumes binding of the actinomycin to the outside of the helix.

Fig. 20 DNA-dependent RNA-polymerase holo-enzyme dimer in Tris-buffer pH 7,5. The inner portions of the scattering curves are plotted according to Guinier.

The concentrations c of the solutions and the apparent radii $\tilde{R}$ of gyration obtained are given in the figure. $\tilde{I}$ is the scattered intensity and 2θ the scattering angle.

Fig. 21 DNA-dependent-RNA-polymerase. The values of the apparent radii of gyration, obtained from Fig.20 for the holo-enzyme dimer and from Fig.28 for the core-enzyme, are plotted versus the concentration.

Fig. 22 Comparison of the experimental curve of the holo-enzyme dimer (xxx) with theoretical curves of hollow circular cylinders of the following axial ratios: The ratio inner radius to outer radius was constant, $r_i/r_a = 0{,}2$, while the ratio v height to outer diameter $v = h/2r_a$ was varied from 0,1 to 1,0 as indicated in the figure; $s = \frac{4\pi}{\lambda} \sin\theta$.

Fig. 23 Comparison of the experimental curve of the holo-enzyme dimer (xxx) with theoretical curves of hollow circular cylinders of the following axial ratios: The ratio height to outer diameter was constant, $v = h/2r_a = 0{,}4$. Varied was the ratio inner radius to outer radius r_i/r_a from 0 (full cylinder) to 0,5; $s = \frac{4\pi}{\lambda} \sin\theta$.

Fig. 24 Comparison of the experimental curve of the holo-enzyme dimer (xxx) with theoretical curves of hollow circular cylinders of the following axial ratios: The ratio height to outer diameter was constant, $v = h/2r_a = 0{,}4$. The ratio inner radius to outer radius r_i/r_a was varied from 0,1 to 0,3.

Fig. 25 DNA-dependent RNA-polymerase in Tris-buffer +0,5 M K Cl at pH 7,4. The inner portions of the scattering curves

are plotted according to Guinier. The concentrations c of the solutions and the apparent radii $\tilde{R}$ of gyration obtained are given in the figure.

Fig. 26 Slit-smeared scattering curves of the DNA-dependent RNA-polymerase in Guinier plot. The radii of gyration obtained are given in the figure.

Fig. 27 Log-log plot of the scattering curve of the holo-enzyme at high ionic strength; $s = \frac{4\pi}{\lambda} \sin\theta$.

Fig. 28 DNA-dependent RNA-Polymerase (Core-enzyme) in Tris-buffer +0,5 NH_4Cl at pH 7,4. The inner portions of the scattering curves are plotted according to Guinier. The concentrations c of the solutions and the apparent radii $\tilde{R}$ of gyration obtained are given in the figure.

Fig. 29 Log-log plot of the scattering curve of the Core-enzyme. $s = \frac{4\pi}{\lambda} \sin\theta$.

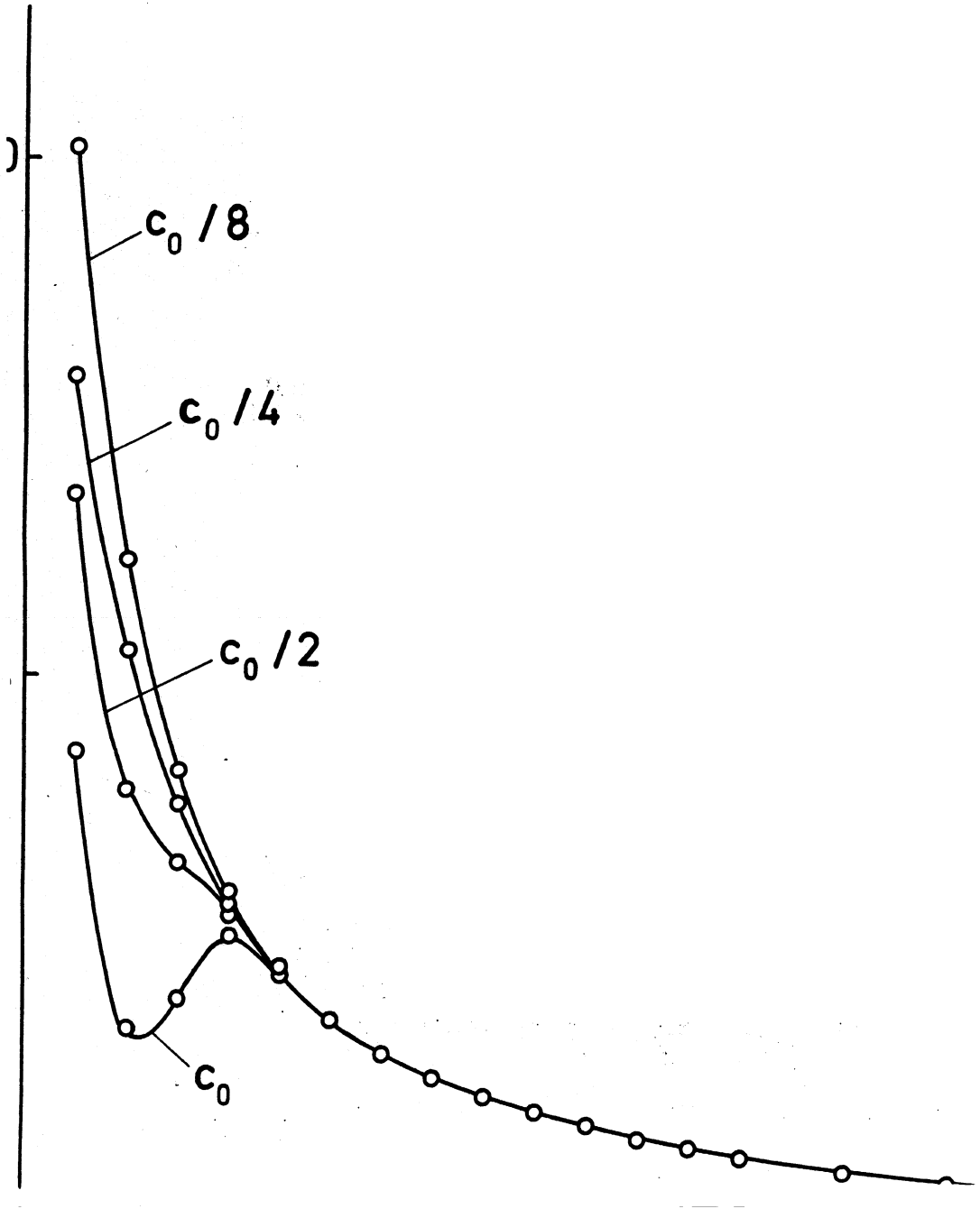
$c_0/8$
$c_0/4$
$c_0/2$
c_0

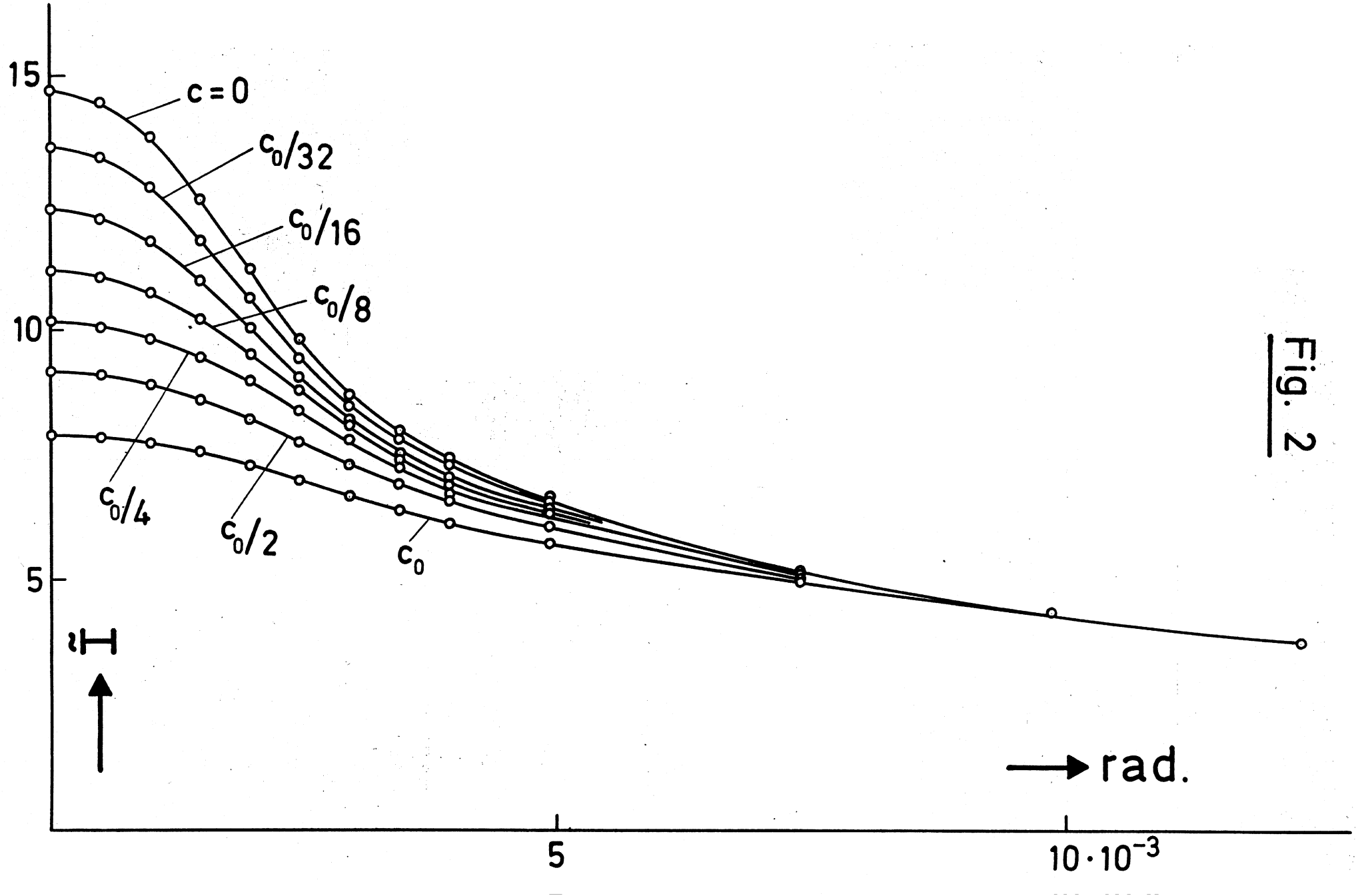

Fig. 2

Fig. 3

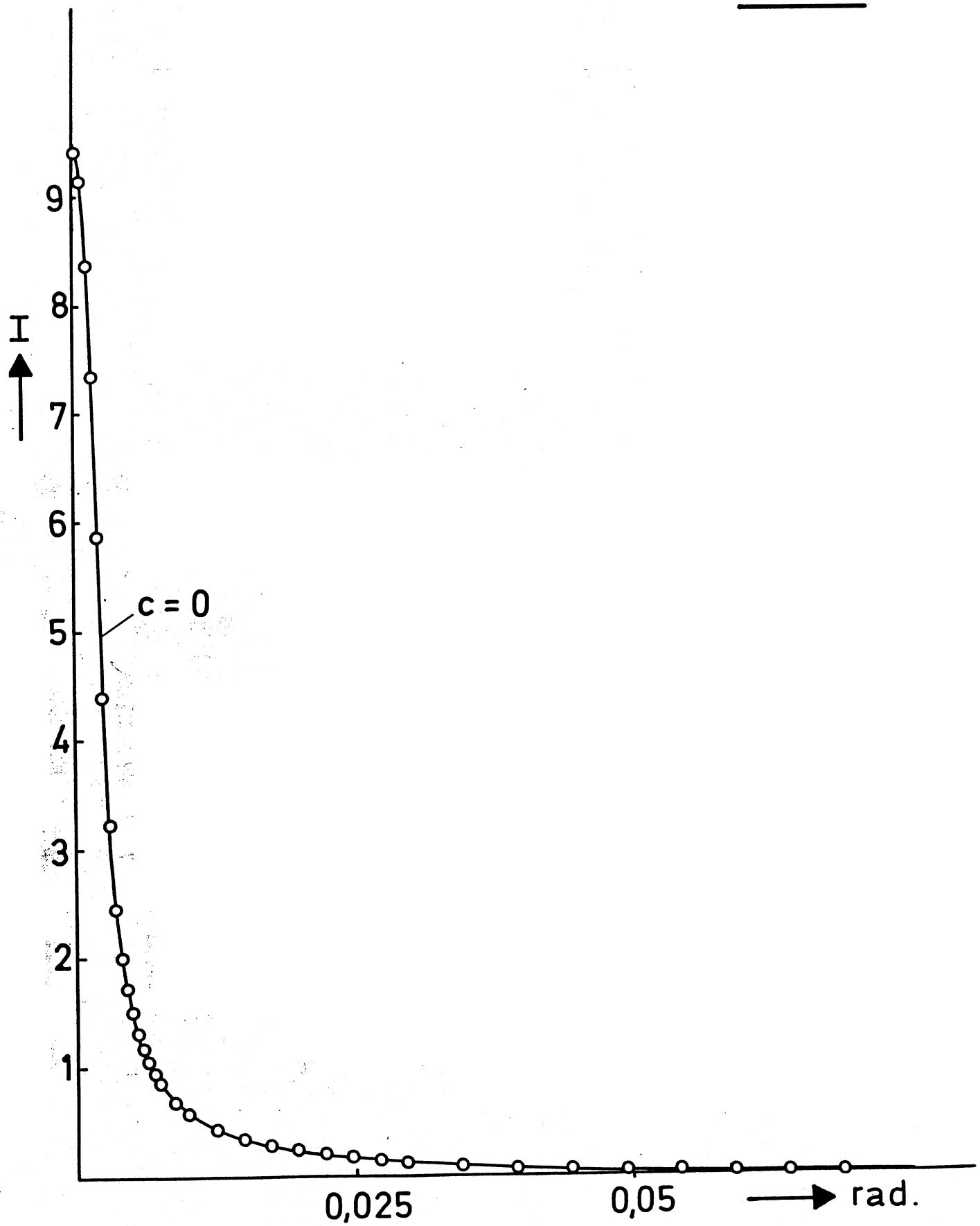

Fig. 4

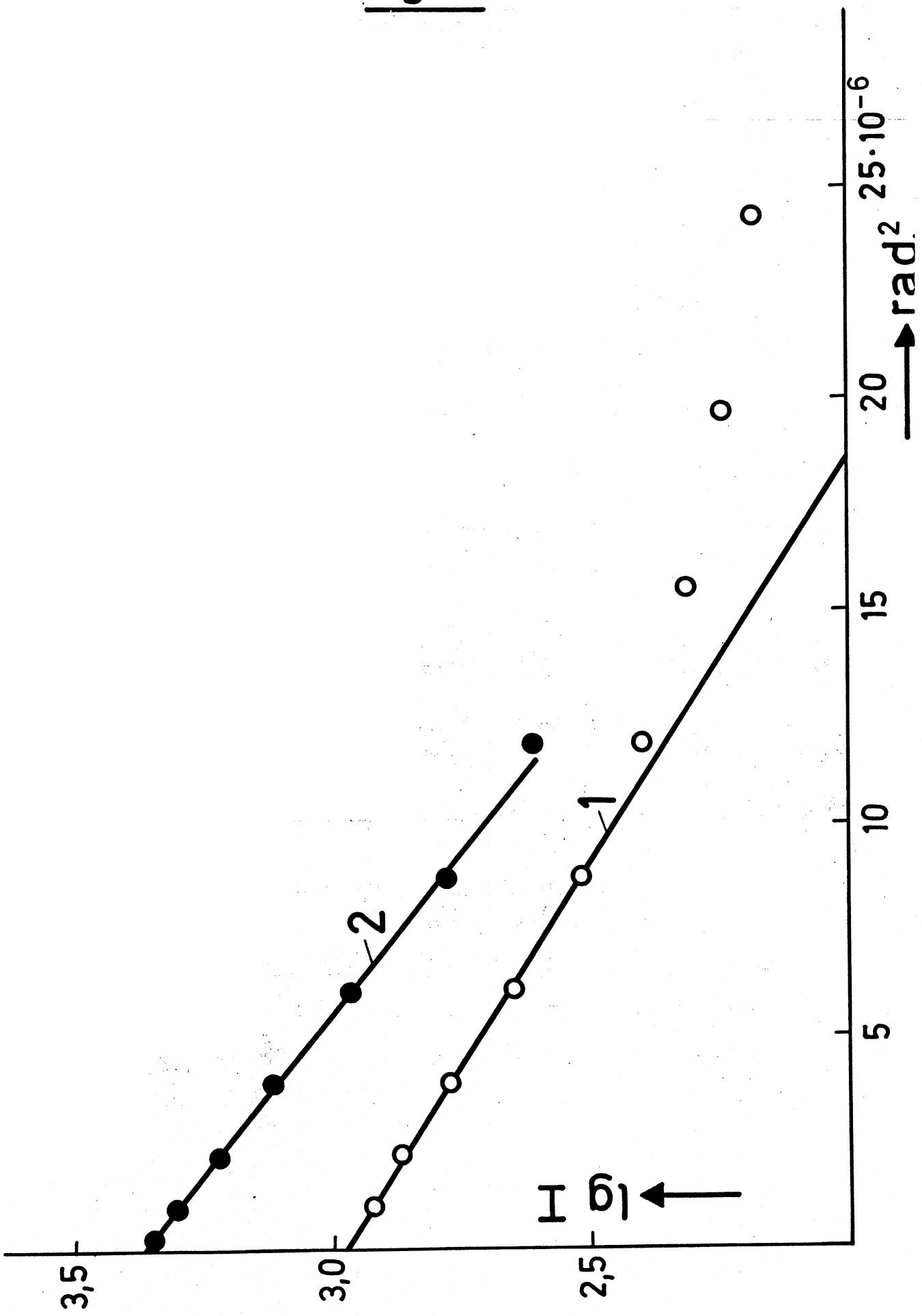

Fig. 5